Error Analysis of a Decoupled Finite Element Method for Quad-Curl Problems

Shuhao Cao[1] · Long Chen[2] · Xuehai Huang[3]

© The Author(s), under exclusive licence to Springer Science+Business Media, LLC, part of Springer Nature 2021

Abstract

Finite element approximation to a decoupled formulation for the quad-curl problem is studied in this paper. The difficulty of constructing elements with certain conformity to the quad–curl problems has been greatly reduced. For convex domains, where the regularity assumption holds for Stokes equation, the approximation to the curl of the true solution has quadratic order of convergence and first order for the energy norm. If the solution shows singularity, an a posterior error estimator is developed and a separate marking adaptive finite element procedure is proposed, together with its convergence proved. Both the a priori and a posteriori error analysis are supported by the numerical examples.

Keywords Quad-curl problem · Decoupled formulation · A posteriori error estimator · Adaptive finite element methods

Mathematics Subject Classification 65N30 · 65N12 · 65N22 · 65N50

✉ Xuehai Huang
huang.xuehai@sufe.edu.cn

Shuhao Cao
s.cao@wustl.edu

Long Chen
chenlong@math.uci.edu

[1] Department of Mathematics and Statistics, Washington University, St. Louis, MO 63130, USA

[2] Department of Mathematics, University of California at Irvine, Irvine, CA 92697, USA

[3] School of Mathematics, Shanghai University of Finance and Economics, Shanghai 200433, China

1 Introduction

Quad-curl problem arises from multiphysics simulation such as modeling a magnetized plasma in magnetohydrodynamics (MHD). In both limiting regimes, resistive MHD [5,47] and electron MHD [13,33,44], discretizing the quad-curl operator is one of the keys to simulate these models. In the meantime, quad-curl operator also plays an important role in approximating the Maxwell transmission eigenvalue problem [12,36]. Recently, the designing of the approximations for quad-curl problems gain quite a few attentions from the finite element community. For example, conforming finite element spaces for the quad-curl problem has been recently constructed in [28,51] in two dimensions and [27,39,52] in three dimensions. Nonconforming and low order finite element spaces can be found in [30,55]. The mixed methods are studied in [45,49,53]. A formulation based on the Hodge decomposition is in [10]. A discontinuous Galerkin approach is studied in [25]. In [46], a novel weak Galerkin formulation exploits the conforming space for curl-curl problem as a nonconforming space for the quad-curl problem. The a posteriori error analysis in two dimensions is studied in [50]. We also refer to [54] for a virtual element method in two dimensions.

The structures of the quad-curl problem are unique as the operator may have a bigger kernel than the one in the curl-curl problem. In a simply-connected domain, the weak formulation of the quad-curl problem is equivalent to that with a grad curl operator [3,53]. Consequently, the stringent continuity condition of the grad curl drives the local polynomial space's dimension to be much bigger than that of the curl-curl problem. This poses extra difficulty in constructing the conforming finite element approximations, and renders them hard to solve especially in three dimensions. The nonconforming elements [55] greatly simply the local structure of the space, and is more preferable in approximating the quad-curl problem in terms of the computational resources.

In [15,30], a novel way of further simplifying the structure of the quad-curl problem is proposed. The quad-curl problem is decoupled into three sub-problems, two curl-curl equations, and one Stokes equation, all of which have mature finite element approximation theories (e.g., [20,31,32,37]). In this paper, we use lower-order Nédélec elements [37,38] to discretize curl-curl equations, and the nonconforming P_1-P_0 finite element to discretize Stokes equation, then analyze this decoupled finite element method (FEM) for the quad-curl problem. Due to the decoupling mechanism, one of the major advantages is that the curl of the primal variable can be approximated an order higher than most of the conforming or nonconforming FEMs.

Meanwhile, due to the nature of quad-curl operator [40], on a polyhedral domain, the singularities of solution may manifest themselves as either corner singularities of the Stokes system with Dirichlet boundary conditions, corner/edge singularities of the Maxwell problem, or both. To cope with such solutions with the presence of singularities, adaptive finite element method (AFEM) is favored over the finite element method performed on a uniformly refined mesh. The computational resources are adaptively allocated throughout different locations of the mesh based on the local estimated approximation error. Thus the AFEM can achieve the same overall accuracy while using fewer degrees of freedom than the one with uniform mesh.

Opting for a decoupled system using existing and mature elements for each offers great facilitation to the AFEM pipeline. Now there are three major pieces to the puzzle: the a posteriori error estimation for the conforming approximation to the Maxwell problem (e.g., [4,11,19,42]), that for a nonconforming discretization to the Stokes problem (e.g., [21,22,48]), and the design of a convergent AFEM algorithm ([26,57,58]). In this paper, combining the

ingredients from both conforming and nonconforming methods, we are able to show that the AFEM algorithm based on the a posteriori error estimation is convergent under common assumptions. Since the nonconforming P_1-P_0 finite element is element-wisely divergence free, as a result, the a posteriori error estimator only involves the discrete velocity, not the discrete pressure. To the best of our knowledge, this paper is the first work to prove the convergence of an adaptive finite element method of the quad-curl problem. Additionally, in terms of solving the resulting linear systems, the biggest advantage of the decoupled formulation is to allow users taking advantage of the existing fast solvers for Stokes and Maxwell problems.

This paper is organized as follows: Section 2 introduces the decoupled formulation as well as its well-posedness. Section 3 proves the a priori error estimation in both the energy norm and the L^2-norm. Section 4 gives the a posteriori error analysis, Sect. 5 shows the quasi-orthogonality of the solution, and a convergence proof is given in Sect. 6. In Sect. 7 a comparison of the rates of convergence of the AFEMs using various marking strategies is presented.

2 A Quad-Curl Problem and a Decoupled Formulation

Let $\Omega \subset \mathbb{R}^3$ be a polyhedron homomorphic to a ball, and $\boldsymbol{f} \in \boldsymbol{H}(\text{div}, \Omega)$ with div $\boldsymbol{f} = 0$. Consider the quad-curl problem

$$\begin{cases} (\text{curl})^4 \boldsymbol{u} = \boldsymbol{f} & \text{in } \Omega, \\ \text{div}\,\boldsymbol{u} = 0 & \text{in } \Omega, \\ \boldsymbol{u} \times \boldsymbol{n} = (\text{curl}\,\boldsymbol{u}) \times \boldsymbol{n} = \boldsymbol{0} & \text{on } \partial\Omega. \end{cases} \tag{2.1}$$

The primal formulation of the quad-curl problem (2.1) is to find $\boldsymbol{u} \in \boldsymbol{H}_0(\text{curl curl}, \Omega)$ such that

$$(\text{curl curl}\,\boldsymbol{u}, \text{curl curl}\,\boldsymbol{v}) = (\boldsymbol{f}, \boldsymbol{v}) \quad \forall\, \boldsymbol{v} \in \boldsymbol{H}_0(\text{curl curl}, \Omega), \tag{2.2}$$

where by denoting $\Gamma := \partial\Omega$

$$\begin{aligned} \boldsymbol{H}_0(\text{curl curl}, \Omega) := \{\boldsymbol{v} \in \boldsymbol{L}^2(\Omega, \mathbb{R}^3) : \text{curl}\,\boldsymbol{v}, \ \text{curl curl}\,\boldsymbol{v} \in \boldsymbol{L}^2(\Omega, \mathbb{R}^3), \\ \text{div}\,\boldsymbol{v} = 0, \ \text{and } \boldsymbol{v} \times \boldsymbol{n} = (\text{curl}\,\boldsymbol{v}) \times \boldsymbol{n} = \boldsymbol{0} \text{ on } \Gamma\}. \end{aligned} \tag{2.3}$$

Here we remark that $H_0(\text{curl curl}, \Omega)$ is same as $H_0(\text{grad curl}, \Omega)$. This is because curl $\boldsymbol{v} \in \boldsymbol{H}_0^1(\Omega, \mathbb{R}^3)$ is equivalent to curl $\boldsymbol{v} \in \boldsymbol{H}_0(\text{curl}, \Omega) \cap \boldsymbol{H}_0(\text{div}, \Omega)$; see [24,53].

A natural mixed method is to mimic the biharmonic equation by introducing $\boldsymbol{w} = \nabla \times \nabla \times \boldsymbol{u}$ and write as a system for which standard edge elements can be used; see [45]. The main drawback of this decoupling is the loss of the order of convergence due to the fact that boundary condition $(\text{curl}\,\boldsymbol{u}) \times \boldsymbol{n} = \boldsymbol{0}$ is imposed weakly. Indeed a natural space for $\boldsymbol{w}$ is $\boldsymbol{H}^{-1}(\text{curl curl}, \Omega) := \{\boldsymbol{v} \in \boldsymbol{L}^2(\Omega; \mathbb{R}^3) : \text{curl curl}\,\boldsymbol{v} \in \boldsymbol{H}^{-1}(\text{div}, \Omega)\}$. Here $\boldsymbol{H}^{-1}(\text{div}, \Omega) := \{\boldsymbol{v} \in \boldsymbol{H}^{-1}(\Omega; \mathbb{R}^3) : \text{div}\,\boldsymbol{v} \in \boldsymbol{H}^{-1}(\Omega)\}$ is the dual space of $\boldsymbol{H}_0(\text{curl}, \Omega)$ [15]. Also inheriting from decoupling the biharmonic equation, fast solvers for the linear algebraic system arising from this discretization could be an issue.

Instead we shall consider a decoupling [15, Section 3.4] (see also [53]) so that the optimal order of convergence can be preserved, and meanwhile the solution can be computed efficiently. More importantly, for solutions with singularities, the a posteriori error analysis and adaptive finite element methods can be applied to retain optimal order of convergence which is the focus of this work.

Introduce the space

$$K_0^c := \{\boldsymbol{\phi} \in \boldsymbol{H}_0(\text{curl}, \Omega) : \text{div}\boldsymbol{\phi} = 0\} = \boldsymbol{H}_0(\text{curl}, \Omega)/\text{grad}\, H_0^1(\Omega)$$

equipped with norm $\|\cdot\|_{H(\text{curl})}$. Due to the following commutative diagram

$$
\begin{array}{ccc}
\boldsymbol{H}_0^1(\Omega; \mathbb{R}^3) & \xrightarrow{\Delta} & \boldsymbol{H}^{-1}(\Omega; \mathbb{R}^3) \\
& & \cup \\
L_0^2(\Omega) \xrightarrow{\text{grad}} & \boldsymbol{H}^{-1}(\text{curl}, \Omega) \xrightarrow{\text{curl}} & (K_0^c)' \longrightarrow 0 \\
& I \uparrow & \uparrow \text{curl curl} \\
& \boldsymbol{H}_0(\text{div}, \Omega) \xleftarrow{\text{curl}} & K_0^c
\end{array}
, $$

the primal formulation (2.2) of the quad-curl problem can be decoupled into the following three systems [15, Section 3.4] (see also [53]):

Step 1. Given $\boldsymbol{f} \in \boldsymbol{L}^2(\Omega)$, find $\boldsymbol{w} \in \boldsymbol{H}_0(\text{curl}, \Omega)$, $\sigma \in H_0^1(\Omega)$ s.t.

$$(\text{curl}\, \boldsymbol{w}, \text{curl}\, \boldsymbol{v}) + (\boldsymbol{v}, \nabla\sigma) = (\boldsymbol{f}, \boldsymbol{v}) \quad \forall\, \boldsymbol{v} \in \boldsymbol{H}_0(\text{curl}, \Omega), \tag{2.4}$$

$$(\boldsymbol{w}, \nabla\tau) = 0 \quad \forall\, \tau \in H_0^1(\Omega). \tag{2.5}$$

Step 2. Given $\boldsymbol{w}$ computed in Step 1, find $\boldsymbol{\phi} \in \boldsymbol{H}_0^1(\Omega; \mathbb{R}^3)$, $p \in L_0^2(\Omega)$ s.t.

$$(\nabla\boldsymbol{\phi}, \nabla\boldsymbol{\psi}) + (\text{div}\, \boldsymbol{\psi}, p) = (\text{curl}\, \boldsymbol{w}, \boldsymbol{\psi}) \quad \forall\, \boldsymbol{\psi} \in \boldsymbol{H}_0^1(\Omega; \mathbb{R}^3), \tag{2.6}$$

$$(\text{div}\, \boldsymbol{\phi}, q) = 0 \quad \forall\, q \in L_0^2(\Omega). \tag{2.7}$$

Step 3. Given $\boldsymbol{\phi}$ computed in Step 2, find $\boldsymbol{u} \in \boldsymbol{H}_0(\text{curl}, \Omega)$ and $\xi \in H_0^1(\Omega)$ s.t.

$$(\text{curl}\, \boldsymbol{u}, \text{curl}\, \boldsymbol{\chi}) + (\boldsymbol{\chi}, \nabla\xi) = (\boldsymbol{\phi}, \text{curl}\, \boldsymbol{\chi}) \quad \forall\, \boldsymbol{\chi} \in \boldsymbol{H}_0(\text{curl}, \Omega), \tag{2.8}$$

$$(\boldsymbol{u}, \nabla\zeta) = 0 \quad \forall\, \zeta \in H_0^1(\Omega). \tag{2.9}$$

In other words, the primal formulation (2.2) of the quad-curl problem (2.1) can be decoupled into two Maxwell equations and one Stokes equation.

Each system is well-posed and the solution $(\boldsymbol{w}, \sigma, \boldsymbol{\phi}, p, \boldsymbol{u}, \xi)$ to (2.4)-(2.9) exists and is unique. Now we show briefly, without resorting to the abstract framework in [15], the equivalence of the decoupled formulation (2.4)-(2.9) and the primary formulation (2.2).

By taking $\boldsymbol{\chi} = \nabla\xi$ in (2.8), we conclude the Lagrange multiplier $\xi = 0$. Therefore (2.8) becomes $\boldsymbol{\phi} = \text{curl}\, \boldsymbol{u}$. Notice that the boundary condition $\text{curl}\, \boldsymbol{u} \times \boldsymbol{n} = 0$ implies that the tangential trace $\boldsymbol{\phi} \times \boldsymbol{n}$ is zero, while $\boldsymbol{u} \times \boldsymbol{n} = 0$ on boundary implies the normal trace $\boldsymbol{\phi} \cdot \boldsymbol{n} = \text{rot}_\Gamma\, \boldsymbol{u} = 0$. Together with $\text{curl}\, \boldsymbol{\phi} = \text{curl}\, \text{curl}\, \boldsymbol{u} \in \boldsymbol{L}^2(\Omega)$ and $\text{div}\, \boldsymbol{\phi} = 0$, by the embedding $\boldsymbol{H}_0(\text{curl}, \Omega) \cap \boldsymbol{H}_0(\text{div}, \Omega) \hookrightarrow \boldsymbol{H}_0^1(\Omega)$ [41], we conclude that $\boldsymbol{\phi} = \text{curl}\, \boldsymbol{u} \in \boldsymbol{H}_0^1(\Omega)$.

Furthermore by the identity

$$(\nabla\boldsymbol{\phi}, \nabla\boldsymbol{\psi}) = (\text{curl}\, \boldsymbol{\phi}, \text{curl}\, \boldsymbol{\psi}) + (\text{div}\, \boldsymbol{\phi}, \text{div}\, \boldsymbol{\psi}) \quad \forall\, \boldsymbol{\phi}, \boldsymbol{\psi} \in \boldsymbol{H}_0^1(\Omega; \mathbb{R}^3),$$

and $\text{div}\, \boldsymbol{\phi} = 0$, we can rewrite (2.6) as

$$(\text{curl}\, \boldsymbol{\phi}, \text{curl}\, \boldsymbol{\psi}) + (\text{div}\, \boldsymbol{\psi}, p) = (\text{curl}\, \boldsymbol{w}, \boldsymbol{\psi}) \quad \forall\, \boldsymbol{\psi} \in \boldsymbol{H}_0^1(\Omega; \mathbb{R}^3). \tag{2.10}$$

Noticing the fact $\text{div}\, \boldsymbol{f} = 0$, by choosing $\boldsymbol{v} = \nabla\sigma$, we get from (2.4) that the Lagrange multipliers σ is also zero. Now choosing $\boldsymbol{\psi} = \text{curl}\, \boldsymbol{v}$ in (2.10) for a $\boldsymbol{v} \in \boldsymbol{H}_0(\text{curl}\,\text{curl}, \Omega)$, we get

$$(\text{curl}\,\text{curl}\, \boldsymbol{u}, \text{curl}\,\text{curl}\, \boldsymbol{v}) = (\text{curl}\, \boldsymbol{\phi}, \text{curl}\, \boldsymbol{\psi}) = (\text{curl}\, \boldsymbol{w}, \boldsymbol{\psi}) = (\boldsymbol{f}, \boldsymbol{v}),$$

which verifies that the solution $\boldsymbol{u}$ to (2.8)-(2.9) is also the solution to (2.2) and vice versa.

Remark 2.1 The decoupled formulation (2.4)-(2.9) also works for the case div $\boldsymbol{f} \neq 0$. By taking $\boldsymbol{v} = \nabla \tau$ in (2.4), we get $\Delta \sigma = $ div $\boldsymbol{f}$. After deriving σ, we can simply replace the right hand side $\boldsymbol{f}$ by $\boldsymbol{f} - \nabla \sigma$, which is divergence-free. This is a Helmholtz decomposition where the non-compatible right-hand side's divergence has been taken into account without being explicitly formulated.

Remark 2.2 As we have shown the auxiliary function $\boldsymbol{\phi} = $ curl $\boldsymbol{u}$, but $\boldsymbol{w} \neq $ curl curl $\boldsymbol{u}$. Equation (2.4) can be equivalently written as curl curl $\boldsymbol{w} = \boldsymbol{f}$ but now $\boldsymbol{w} \in \boldsymbol{H}_0(\text{curl}, \Omega)$ while curl curl $\boldsymbol{u} \in \boldsymbol{H}_0(\text{div}, \Omega)$ may not satisfy the tangential boundary condition.

3 Discrete Methods and a Priori Error Analysis

We consider a conforming mixed finite element method of the Maxwell equations (2.4)-(2.5), and (2.8)-(2.9) but a nonconforming method for Stokes equation (2.6)-(2.7). We refer to [53] for a conforming mixed finite element method.

Let $\{\mathcal{T}_h\}$ be a family of triangulation of Ω with mesh size $h = \max_{K \in \mathcal{T}_h} h_K$, where h_K is the diameter of the tetrahedron K. Denote the p-th order Lagrange element space by

$$V_h^p := \{v_h \in H_0^1(\Omega) : v_h|_K \in \mathbb{P}_p(K) \text{ for each } K \in \mathcal{T}_h\},$$

and the lowest-order Nédélec edge element space [37] by

$$\boldsymbol{V}_h^c := \{\boldsymbol{v}_h \in \boldsymbol{H}_0(\text{curl}, \Omega) : \boldsymbol{v}_h|_K \in \mathbb{P}_0(K; \mathbb{R}^3) \oplus \boldsymbol{x} \wedge \mathbb{P}_0(K; \mathbb{R}^3) \text{ for each } K \in \mathcal{T}_h\}.$$

We use $V_h^1 - \boldsymbol{V}_h^c$ to discretize the Maxwell equation (2.4)-(2.5). Find $\boldsymbol{w}_h \in \boldsymbol{V}_h^c$, $\sigma_h \in V_h^1$ s.t.

$$(\text{curl } \boldsymbol{w}_h, \text{curl } \boldsymbol{v}_h) + (\boldsymbol{v}_h, \nabla \sigma_h) = (\boldsymbol{f}, \boldsymbol{v}_h) \quad \forall \boldsymbol{v}_h \in \boldsymbol{V}_h^c, \tag{3.1}$$

$$(\boldsymbol{w}_h, \nabla \tau_h) = 0 \quad \forall \tau_h \in V_h^1. \tag{3.2}$$

We then use the nonconforming P_1-P_0 element [20] to discretize the Stokes problem (2.6)-(2.7). To this end, let

$$\boldsymbol{V}_h^{\text{CR}} := \{\boldsymbol{\psi}_h \in \boldsymbol{L}^2(\Omega; \mathbb{R}^3) : \boldsymbol{\psi}_h|_K \in \mathbb{P}_1(K; \mathbb{R}^3) \text{ for each } K \in \mathcal{T}_h,$$
$$\text{and } ([\![\boldsymbol{\psi}_h]\!], 1)_F = 0 \text{ for each } F \in \mathcal{F}_h\},$$

where $[\![\boldsymbol{v}]\!](\boldsymbol{x}) := \lim_{\epsilon \to 0^+} \left(\boldsymbol{v}|_{K_1}(\boldsymbol{x} - \epsilon \boldsymbol{n}_{K_1}) - \boldsymbol{v}|_{K_2}(\boldsymbol{x} + \epsilon \boldsymbol{n}_{K_1}) \right)$ is defined as the jump on face F for $\boldsymbol{x} \in F$ and $\boldsymbol{n}_{K_1}$ being the outer unit normal to K_1 on face F. Denote the piecewise constant space as

$$\mathcal{Q}_h := \{q_h \in L_0^2(\Omega) : q_h|_K \in \mathbb{P}_0(K) \text{ for each } K \in \mathcal{T}_h\}.$$

Given $\boldsymbol{w}_h$ computed from (3.1)-(3.2), find $\boldsymbol{\phi}_h \in \boldsymbol{V}_h^{\text{CR}}$, $p_h \in \mathcal{Q}_h$ s.t.

$$(\nabla_h \boldsymbol{\phi}_h, \nabla_h \boldsymbol{\psi}_h) + (\text{div}_h \boldsymbol{\psi}_h, p_h) = (\text{curl } \boldsymbol{w}_h, \boldsymbol{\psi}_h) \quad \forall \boldsymbol{\psi}_h \in \boldsymbol{V}_h^{\text{CR}}, \tag{3.3}$$

$$(\text{div}_h \boldsymbol{\phi}_h, q_h) = 0 \quad \forall q_h \in \mathcal{Q}_h. \tag{3.4}$$

Hereafter ∇_h, curl_h and div_h mean the element-wise defined counterparts of ∇, curl and div with respect to $\mathcal{T}_h$.

Upon solving the system above, $\boldsymbol{\phi}_h$ is a second-order approximation to curl $\boldsymbol{u}$ when the data is smooth. Finally, when one needs to seek a better approximation to $\boldsymbol{u}$ under L^2-norm, $\boldsymbol{u}_h \in \boldsymbol{V}_h^{c_1}$ and $\xi_h \in V_h^2$ are sought such that they satisfy

$$(\text{curl } \boldsymbol{u}_h, \text{curl } \boldsymbol{\chi}_h) + (\boldsymbol{\chi}_h, \nabla \xi_h) = (\boldsymbol{\phi}_h, \text{curl } \boldsymbol{\chi}_h) \quad \forall \, \boldsymbol{\chi}_h \in \boldsymbol{V}_h^{c_1}, \tag{3.5}$$

$$(\boldsymbol{u}_h, \nabla \zeta_h) = 0 \quad \forall \, \zeta_h \in V_h^2. \tag{3.6}$$

Here $\boldsymbol{V}_h^{c_1}$ is the linear second family of Nédélec element:

$$\boldsymbol{V}_h^{c_1} := \{\boldsymbol{v}_h \in \boldsymbol{H}_0(\text{curl}, \Omega) : \boldsymbol{v}_h|_K \in \mathbb{P}_1(K; \mathbb{R}^3) \text{ for each } K \in \mathcal{T}_h\},$$

and V_h^2 is the quadratic Lagrange element.

The finite element pair $(\boldsymbol{V}_h^{\text{CR}}, \mathcal{Q}_h)$ is stable for the Stokes equation [6], i.e., we have for any $\widetilde{\boldsymbol{\phi}}_h \in \boldsymbol{V}_h^{\text{CR}}$ and $\widetilde{p}_h \in \mathcal{Q}_h$ that

$$|\widetilde{\boldsymbol{\phi}}_h|_{1,h} + \|\widetilde{p}_h\|_0 \lesssim \sup_{\substack{\boldsymbol{\psi}_h \in \boldsymbol{V}_h^{\text{CR}} \\ q_h \in \mathcal{Q}_h}} \frac{(\nabla_h \widetilde{\boldsymbol{\phi}}_h, \nabla_h \boldsymbol{\psi}_h) + (\text{div}_h \, \boldsymbol{\psi}_h, \widetilde{p}_h) + (\text{div}_h \, \widetilde{\boldsymbol{\phi}}_h, q_h)}{|\boldsymbol{\psi}_h|_{1,h} + \|q_h\|_0}.$$

3.1 A Priori Error Analysis

Next we focus on the a priori error analysis for the decoupled mixed finite element method (3.1)-(3.6). First of all, since div $\boldsymbol{f} = 0$ and $\nabla V_h^1 \subset \boldsymbol{V}_h^c$, we get from (3.1) and (3.5) that $\sigma_h = 0$ and $\xi_h = 0$.

Lemma 3.1 (Galerkin orthogonality) *Let* $(\boldsymbol{w}, 0) \in \boldsymbol{H}_0(\text{curl}, \Omega) \times H_0^1(\Omega)$ *be the solution of the Maxwell equation* (2.4)–(2.5)*, and* $(\boldsymbol{w}_h, 0) \in \boldsymbol{V}_h^c \times V_h^1$ *be the solution of the mixed method* (3.1)–(3.2)*. Then*

$$(\text{curl}(\boldsymbol{w} - \boldsymbol{w}_h), \text{curl } \boldsymbol{v}_h) = 0 \quad \forall \, \boldsymbol{v}_h \in \boldsymbol{V}_h^c. \tag{3.7}$$

Proof As the Lagrange multiplier $\sigma = 0$ and its approximation $\sigma_h = 0$, subtracting (3.1) from (2.4), we get the desired orthogonality. □

The error analysis of the mixed finite element method (3.1)-(3.2) is first studied by F. Kikuchi in [31,32]. We recall it for completeness.

Lemma 3.2 *Let* $(\boldsymbol{w}, 0) \in \boldsymbol{H}_0(\text{curl}, \Omega) \times H_0^1(\Omega)$ *be the solution of the Maxwell equation* (2.4)-(2.5)*, and* $(\boldsymbol{w}_h, 0) \in \boldsymbol{V}_h^c \times V_h^1$ *the solution of the mixed method* (3.1)-(3.2)*. Assume* curl $\boldsymbol{w} \in \boldsymbol{H}^1(\Omega; \mathbb{R}^3)$*, then we have*

$$\|\text{curl}(\boldsymbol{w} - \boldsymbol{w}_h)\|_0 \lesssim h|\text{curl } \boldsymbol{w}|_1. \tag{3.8}$$

Proof The orthogonality (3.7) implies the best approximation

$$\|\text{curl}(\boldsymbol{w} - \boldsymbol{w}_h)\|_0 \leq \inf_{\boldsymbol{v}_h \in \boldsymbol{V}_h^c} \|\text{curl}(\boldsymbol{w} - \boldsymbol{v}_h)\|_0.$$

This gives (3.8) by an interpolation error estimate (see e.g., [35]). □

According to the Poincaré-Friedrichs inequality for piecewise H^1 functions [8], the following inequality holds

$$\|\psi_h\|_0 \lesssim |\psi_h|_{1,h} \quad \forall \, \psi_h \in \boldsymbol{V}_h^{\text{CR}} + \boldsymbol{H}_0^1(\Omega; \mathbb{R}^3).$$

Denote $\boldsymbol{I}_h^s$ as the nodal interpolation operator from $\boldsymbol{H}_0^1(\Omega; \mathbb{R}^3)$ to $\boldsymbol{V}_h^{\mathrm{CR}}$, then

$$(\nabla(\boldsymbol{\psi} - \boldsymbol{I}_h^s \boldsymbol{\psi}), \boldsymbol{\tau})_K = 0 \quad \forall \, \boldsymbol{\psi} \in \boldsymbol{H}^1(\Omega; \mathbb{R}^3), \boldsymbol{\tau} \in \mathbb{P}_0(K; \mathbb{M}), \quad K \in \mathcal{T}_h, \qquad (3.9)$$

where $P_0(K; \mathbb{M})$ stands for the space of constant 3×3 matrix on K, and for $j = 1, 2$,

$$\|\boldsymbol{\psi} - \boldsymbol{I}_h^s \boldsymbol{\psi}\|_{0,K} + h_K |\boldsymbol{\psi} - \boldsymbol{I}_h^s \boldsymbol{\psi}|_{1,K} \lesssim h_K^j |\boldsymbol{\psi}|_{j,K} \quad \forall \, \boldsymbol{\psi} \in \boldsymbol{H}^j(\Omega; \mathbb{R}^3), \quad K \in \mathcal{T}_h. \tag{3.10}$$

The error analysis for the nonconforming P_1-P_0 element approximation (3.3)–(3.4) of Stokes equation is standard [20]. Using the decoupled system to approximate the quad–curl problem, the subtlety is the perturbation of data. We shall present a stability result for using curl $\boldsymbol{w}_h$ to approximate curl $\boldsymbol{w}$. To this end, we introduce the space

$$\boldsymbol{Z} := \boldsymbol{H}_0^1(\Omega; \mathbb{R}^3) \cap \ker(\mathrm{div}).$$

Subsequently (2.6) and the continuous problem using the perturbed data can be written as follows:

$$-\Delta \boldsymbol{\phi} = \mathrm{curl} \, \boldsymbol{w} \text{ in } \boldsymbol{Z}' \quad \text{and} \quad -\Delta \tilde{\boldsymbol{\phi}} = \mathrm{curl} \, \boldsymbol{w}_h \text{ in } \boldsymbol{Z}',$$

respectively. The second problem above is equivalent to

$$(\nabla \tilde{\boldsymbol{\phi}}, \nabla \boldsymbol{\psi}) + (\mathrm{div} \, \boldsymbol{\psi}, \tilde{p}) = (\mathrm{curl} \, \boldsymbol{w}_h, \boldsymbol{\psi}) \quad \forall \, \boldsymbol{\psi} \in \boldsymbol{H}_0^1(\Omega; \mathbb{R}^3), \tag{3.11}$$

$$(\mathrm{div} \, \tilde{\boldsymbol{\phi}}, q) = 0 \quad \forall \, q \in L_0^2(\Omega). \tag{3.12}$$

The analysis is performed for this problem with the perturbed data.

Lemma 3.3 *Let* $(\boldsymbol{\phi}, p)$, $(\tilde{\boldsymbol{\phi}}, \tilde{p})$ *be the solutions to* (2.6)–(2.7) *and* (3.11)–(3.12), *respectively, where* $\boldsymbol{w}$ *and* $\boldsymbol{w}_h$ *satisfy the orthogonality* (3.7). *Then*

$$\|\tilde{\boldsymbol{\phi}} - \boldsymbol{\phi}\|_1 \lesssim h \| \mathrm{curl}(\boldsymbol{w} - \boldsymbol{w}_h)\|_0.$$

Proof The difference between the two pairs satisfies the Stokes equation

$$-\Delta(\boldsymbol{\phi} - \tilde{\boldsymbol{\phi}}) + \nabla(p - \tilde{p}) = \mathrm{curl}(\boldsymbol{w} - \boldsymbol{w}_h) \quad \text{in } (\boldsymbol{H}_0^1(\Omega; \mathbb{R}^3))',$$

$$\mathrm{div}(\boldsymbol{\phi} - \tilde{\boldsymbol{\phi}}) = 0 \quad \text{in } L_0^2(\Omega).$$

Applying the definition of the duality pair testing against $\boldsymbol{\phi} - \tilde{\boldsymbol{\phi}}$, we get

$$|\boldsymbol{\phi} - \tilde{\boldsymbol{\phi}}|_1^2 = (\mathrm{curl}(\boldsymbol{w} - \boldsymbol{w}_h), \boldsymbol{\phi} - \tilde{\boldsymbol{\phi}}).$$

Moreover, since $\mathrm{div}(\boldsymbol{\phi} - \tilde{\boldsymbol{\phi}}) = 0$, by [24, Chapter 1 Theorem 3.4] there exists $\boldsymbol{v} \in \boldsymbol{H}_0^1(\Omega; \mathbb{R}^3)$ such that

$$\boldsymbol{\phi} - \tilde{\boldsymbol{\phi}} = \mathrm{curl} \, \boldsymbol{v}, \quad \|\boldsymbol{v}\|_1 \lesssim \|\boldsymbol{\phi} - \tilde{\boldsymbol{\phi}}\|_0.$$

Then it follows from (3.7) that

$$|\boldsymbol{\phi} - \tilde{\boldsymbol{\phi}}|_1^2 = (\mathrm{curl}(\boldsymbol{w} - \boldsymbol{w}_h), \mathrm{curl} \, \boldsymbol{v}) = (\mathrm{curl}(\boldsymbol{w} - \boldsymbol{w}_h), \mathrm{curl}(\boldsymbol{v} - \boldsymbol{v}_h)), \quad \forall \, \boldsymbol{v}_h \in \boldsymbol{V}_h^c.$$

Thus

$$|\boldsymbol{\phi} - \tilde{\boldsymbol{\phi}}|_1^2 \leq \| \mathrm{curl}(\boldsymbol{w} - \boldsymbol{w}_h)\|_0 \inf_{\boldsymbol{v}_h \in \boldsymbol{V}_h^c} \| \mathrm{curl}(\boldsymbol{v} - \boldsymbol{v}_h)\|_0 \lesssim h \| \mathrm{curl}(\boldsymbol{w} - \boldsymbol{w}_h)\|_0 |\boldsymbol{\phi} - \tilde{\boldsymbol{\phi}}|_1,$$

which implies the desired result. □

In the next step, we treat $\boldsymbol{\phi}_h$ as the approximation of $\tilde{\boldsymbol{\phi}}$ and use the standard error analysis to obtain the following estimate. Here the H^2-regularity of Stokes equation is assumed to hold.

(H2) Given an $\boldsymbol{f} \in L^2(\Omega; \mathbb{R}^3)$, let $\boldsymbol{u} \in \boldsymbol{H}_0^1(\Omega; \mathbb{R}^3)$ and $p \in L_0^2(\Omega)$ be the solution of the Stokes equation

$$-\Delta \boldsymbol{u} + \nabla p = \boldsymbol{f}, \quad \text{div } \boldsymbol{u} = 0.$$

Then $\boldsymbol{u} \in \boldsymbol{H}^2(\Omega; \mathbb{R}^3)$ and $p \in H^1(\Omega)$ and

$$\|\boldsymbol{u}\|_2 + \|p\|_1 \lesssim \|f\|_0.$$

It is well known that the assumption (H2) holds for smooth or convex domain Ω (e.g., see [34, Section 11.5]). In particular, assuming (H2) holds, we have

$$\|\boldsymbol{\phi}\|_2 + \|p\|_1 \lesssim \|\text{curl } \boldsymbol{w}\|_0, \quad \|\tilde{\boldsymbol{\phi}}\|_2 + \|\tilde{p}\|_1 \lesssim \|\text{curl } \boldsymbol{w}_h\|_0,$$

thus the standard a priori estimate for the stable nonconforming P_1-P_0 pair holds.

Theorem 3.4 *Let* $(\boldsymbol{\phi}, p) \in \boldsymbol{H}_0^1(\Omega; \mathbb{R}^3) \times L_0^2(\Omega)$ *be the solution of the Stokes equation* (2.6)-(2.7), *and* $(\boldsymbol{\phi}_h, p_h) \in \boldsymbol{V}_h^{\text{CR}} \times \mathcal{Q}_h$ *the solution of the mixed method* (3.3)-(3.4). *Assume the* H^2-*regularity of Stokes equation, i.e., (H2) holds, then*

$$|\boldsymbol{\phi} - \boldsymbol{\phi}_h|_{1,h} \lesssim h\|\text{curl } \boldsymbol{w}\|_0. \tag{3.13}$$

Proof First by a standard estimate [20], and the elliptic regularity estimate of the approximation $\boldsymbol{\phi}_h$ for the Stokes problem with curl $\boldsymbol{w}_h$ as data, we have

$$|\tilde{\boldsymbol{\phi}} - \boldsymbol{\phi}_h|_{1,h} \lesssim h|\tilde{\boldsymbol{\phi}}|_2 \lesssim h\|\text{curl } \boldsymbol{w}_h\|_0.$$

Furthermore, as $\boldsymbol{w}_h$ is the projection of $\boldsymbol{w}$ to the discrete space in the energy norm, from the orthogonality (3.7), we have $\|\text{curl } \boldsymbol{w}_h\|_0 \le \|\text{curl } \boldsymbol{w}\|_0$. Consequently, the theorem follows from combining the estimate with the ones in Lemma 3.3. □

Remark 3.5 (*Nonhomogeneous boundary conditions*) By a simple density argument we can see that curl $\boldsymbol{u} \cdot \boldsymbol{n} = \text{div}_\Gamma(\boldsymbol{u} \times \boldsymbol{n})$. Consequently, the presence of nonhomogeneous $\boldsymbol{u} \times \boldsymbol{n}$ and/or curl $\boldsymbol{u} \times \boldsymbol{n}$ leads to the necessity of impose compatible Dirichlet boundary conditions with the divergence free condition for problems (2.6)–(2.7), (3.11)–(3.12). Let $\boldsymbol{\phi}_I$ be the standard nodal interpolation in Crouzeix-Raviart element of a sufficiently smooth $\boldsymbol{\phi}$, by a standard decomposition argument we can see that aside from the terms on the right hand side of (3.13), for the nonhomogeneous boundary condition, the estimate should include:

$$|\boldsymbol{\phi} - \boldsymbol{\phi}_I|_{1/2,h,\partial\Omega} := \left(\sum_{F \in \mathcal{F}_h} |\boldsymbol{\phi} - \boldsymbol{\phi}_I|_{1/2,F}^2 \right)^{1/2} \lesssim h|\boldsymbol{\phi}|_2.$$

Next we present the L^2-error estimate for the Stokes equation.

Lemma 3.6 *Let* $(\boldsymbol{w}_h, 0, \boldsymbol{\phi}_h, p_h) \in \boldsymbol{V}_h^c \times V_h^1 \times \boldsymbol{V}_h^{\text{CR}} \times \mathcal{Q}_h$ *be the solution of the mixed method* (3.1)–(3.4) *on triangulation* $\mathcal{T}_h$. *Assume* H^2-*regularity of Stokes equation holds, i.e., (H2) holds, then*

$$\|\boldsymbol{\phi} - \boldsymbol{\phi}_h\|_0 \lesssim h|\boldsymbol{\phi} - \boldsymbol{\phi}_h|_{1,h} + h\|\text{curl}(\boldsymbol{w} - \boldsymbol{w}_h)\|_0 + h^2\|\text{curl } \boldsymbol{w}\|_0. \tag{3.14}$$

Furthermore if curl $\boldsymbol{w} \in \boldsymbol{H}^1(\Omega; \mathbb{R}^3)$, *then we have the second order estimate*

$$\|\boldsymbol{\phi} - \boldsymbol{\phi}_h\|_0 \lesssim h^2\|\text{curl } \boldsymbol{w}\|_1. \tag{3.15}$$

Proof Consider the following dual problem: seek $(\hat{\boldsymbol{\phi}}, \hat{p}) \in \boldsymbol{H}_0^1(\Omega; \mathbb{R}^3) \times L_0^2(\Omega)$ such that

$$
\begin{cases}
-\Delta \hat{\boldsymbol{\phi}} + \nabla \hat{p} = \boldsymbol{\phi} - \boldsymbol{\phi}_h, \\
\quad \text{div} \, \hat{\boldsymbol{\phi}} = 0.
\end{cases}
$$

The H^2-regularity to the problem above (e.g., see [34, Section 11.5]) reads

$$
\|\hat{\boldsymbol{\phi}}\|_2 + \|\hat{p}\|_1 \lesssim \|\boldsymbol{\phi} - \boldsymbol{\phi}_h\|_0. \tag{3.16}
$$

Since $\text{div}_h(\boldsymbol{\phi} - \boldsymbol{\phi}_h) = 0$, it follows

$$
\begin{aligned}
\|\boldsymbol{\phi} - \boldsymbol{\phi}_h\|_0^2 &= (\boldsymbol{\phi} - \boldsymbol{\phi}_h, -\Delta \hat{\boldsymbol{\phi}} + \nabla \hat{p}) \\
&= (\nabla_h(\boldsymbol{\phi} - \boldsymbol{\phi}_h), \nabla \hat{\boldsymbol{\phi}}) + \sum_{K \in \mathcal{T}_h} (\boldsymbol{\phi} - \boldsymbol{\phi}_h, \hat{p}\boldsymbol{n} - \partial_n \hat{\boldsymbol{\phi}})_{\partial K}.
\end{aligned} \tag{3.17}
$$

Employing (3.9) and the fact $\text{div}_h \, \boldsymbol{I}_h^s \hat{\boldsymbol{\phi}} = 0$, we obtain

$$
\begin{aligned}
(\nabla_h(\boldsymbol{\phi} - \boldsymbol{\phi}_h), \nabla \hat{\boldsymbol{\phi}}) &= (\nabla \boldsymbol{\phi}, \nabla \hat{\boldsymbol{\phi}}) - (\nabla_h \boldsymbol{\phi}_h, \nabla_h \boldsymbol{I}_h^s \hat{\boldsymbol{\phi}}) = (\text{curl} \, \boldsymbol{w}, \hat{\boldsymbol{\phi}}) - (\text{curl} \, \boldsymbol{w}_h, \boldsymbol{I}_h^s \hat{\boldsymbol{\phi}}) \\
&= (\text{curl} \, \boldsymbol{w} - \text{curl} \, \boldsymbol{w}_h, \hat{\boldsymbol{\phi}}) + (\text{curl} \, \boldsymbol{w}_h, \hat{\boldsymbol{\phi}} - \boldsymbol{I}_h^s \hat{\boldsymbol{\phi}}).
\end{aligned}
$$

Applying the same argument in Lemma 3.3 by treating $\hat{\boldsymbol{\phi}}$ as a stream function and inserting a curl of its interpolation, we achieve

$$
(\text{curl} \, \boldsymbol{w} - \text{curl} \, \boldsymbol{w}_h, \hat{\boldsymbol{\phi}}) \lesssim h \| \text{curl}(\boldsymbol{w} - \boldsymbol{w}_h)\|_0 |\hat{\boldsymbol{\phi}}|_1.
$$

Besides from (3.10), we have

$$
(\text{curl} \, \boldsymbol{w}_h, \hat{\boldsymbol{\phi}} - \boldsymbol{I}_h^s \hat{\boldsymbol{\phi}}) \lesssim h^2 \| \text{curl} \, \boldsymbol{w}\|_0 |\hat{\boldsymbol{\phi}}|_2.
$$

Hence

$$
(\nabla_h(\boldsymbol{\phi} - \boldsymbol{\phi}_h), \nabla \hat{\boldsymbol{\phi}}) \lesssim h \| \text{curl}(\boldsymbol{w} - \boldsymbol{w}_h)\|_0 |\hat{\boldsymbol{\phi}}|_1 + h^2 \| \text{curl} \, \boldsymbol{w}\|_0 |\hat{\boldsymbol{\phi}}|_2. \tag{3.18}
$$

Due to the continuity condition of Crouzeix-Raviart element, by a standard technique of inserting a constant on each face (e.g., see [9, Chapter 10.3]) we get

$$
\sum_{K \in \mathcal{T}_h} (\boldsymbol{\phi} - \boldsymbol{\phi}_h, \hat{p}\boldsymbol{n} - \partial_n \hat{\boldsymbol{\phi}})_{\partial K} \lesssim h |\boldsymbol{\phi} - \boldsymbol{\phi}_h|_{1,h} (\|\hat{\boldsymbol{\phi}}\|_2 + \|\hat{p}\|_1). \tag{3.19}
$$

Combining (3.17)-(3.19) and (3.16) yields

$$
\|\boldsymbol{\phi} - \boldsymbol{\phi}_h\|_0 \lesssim h |\boldsymbol{\phi} - \boldsymbol{\phi}_h|_{1,h} + h \| \text{curl}(\boldsymbol{w} - \boldsymbol{w}_h)\|_0 + h^2 \| \text{curl} \, \boldsymbol{w}\|_0,
$$

which is (3.14). $\qquad\square$

We now consider the approximation (3.5)–(3.6) of the last Maxwell equation. Due to the inexactness of the data, the orthogonality is lost, but the perturbation is measured in L^2-norm of the difference $\boldsymbol{\phi} - \boldsymbol{\phi}_h$, which is controllable.

Lemma 3.7 *Let* $(\boldsymbol{u}, 0) \in \boldsymbol{H}_0(\text{curl}, \Omega) \times H_0^1(\Omega)$ *be the solution of the Maxwell equation (2.8)-(2.9), and* $(\boldsymbol{u}_h, 0) \in \boldsymbol{V}_h^{c_1} \times V_h^2$ *the solution of the mixed method (3.5)-(3.6), then*

$$
\| \text{curl}(\boldsymbol{u} - \boldsymbol{u}_h)\|_0 \lesssim \|\boldsymbol{\phi} - \boldsymbol{\phi}_h\|_0 + \inf_{\boldsymbol{v}_h \in \boldsymbol{V}_h^c} \| \text{curl}(\boldsymbol{u} - \boldsymbol{v}_h)\|_0. \tag{3.20}
$$

Assume that the H^2-regularity of Stokes equation (H2) holds and $\operatorname{curl} \boldsymbol{w}, \operatorname{curl} \boldsymbol{u} \in \boldsymbol{H}^1(\Omega; \mathbb{R}^3)$, *then*

$$\|\operatorname{curl}(\boldsymbol{u} - \boldsymbol{u}_h)\|_0 \lesssim h^2 |\operatorname{curl} \boldsymbol{w}|_1 + h|\operatorname{curl} \boldsymbol{u}|_1.$$

Proof Subtracting (3.5) from (2.8), we get

$$(\operatorname{curl}(\boldsymbol{u} - \boldsymbol{u}_h), \operatorname{curl} \boldsymbol{\chi}_h) = (\boldsymbol{\phi} - \boldsymbol{\phi}_h, \operatorname{curl} \boldsymbol{\chi}_h) \quad \forall \boldsymbol{\chi}_h \in \boldsymbol{V}_h^{c_1}. \tag{3.21}$$

Taking $\boldsymbol{\chi}_h = \boldsymbol{v}_h - \boldsymbol{u}_h$ with $\boldsymbol{v}_h \in \boldsymbol{V}_h^{c_1}$, we acquire

$$
\begin{aligned}
\|\operatorname{curl}(\boldsymbol{u} - \boldsymbol{u}_h)\|_0^2 &= (\operatorname{curl}(\boldsymbol{u} - \boldsymbol{u}_h), \operatorname{curl}(\boldsymbol{u} - \boldsymbol{u}_h)) \\
&= (\operatorname{curl}(\boldsymbol{u} - \boldsymbol{u}_h), \operatorname{curl}(\boldsymbol{u} - \boldsymbol{v}_h)) + (\boldsymbol{\phi} - \boldsymbol{\phi}_h, \operatorname{curl}(\boldsymbol{v}_h - \boldsymbol{u}_h)) \\
&\leq \|\operatorname{curl}(\boldsymbol{u} - \boldsymbol{u}_h)\|_0 \|\operatorname{curl}(\boldsymbol{u} - \boldsymbol{v}_h)\|_0 \\
&\quad + \|\boldsymbol{\phi} - \boldsymbol{\phi}_h\|_0 (\|\operatorname{curl}(\boldsymbol{u} - \boldsymbol{v}_h)\|_0 + \|\operatorname{curl}(\boldsymbol{u} - \boldsymbol{u}_h)\|_0),
\end{aligned}
$$

which indicates

$$\|\operatorname{curl}(\boldsymbol{u} - \boldsymbol{u}_h)\|_0 \lesssim \|\boldsymbol{\phi} - \boldsymbol{\phi}_h\|_0 + \inf_{\boldsymbol{v}_h \in \boldsymbol{V}_h^{c_1}} \|\operatorname{curl}(\boldsymbol{u} - \boldsymbol{v}_h)\|_0.$$

$\square$

Recall that $\boldsymbol{\phi} = \operatorname{curl} \boldsymbol{u}$ and $\|\boldsymbol{\phi} - \boldsymbol{\phi}_h\|_0$ is at least first order h. Therefore if still merely the lowest order edge element is used in (3.5)–(3.6), no approximation to $\operatorname{curl} \boldsymbol{u}$ better than $\boldsymbol{\phi}_h$ could be obtained. By the duality argument for Stokes equation, the error $\|\boldsymbol{\phi} - \boldsymbol{\phi}_h\|_0$ can be of second order h^2 if the H^2-regularity result holds. As a result in the last Maxwell equation, we opt to use the second family Nédélec element to the improve the L^2 approximation of $\boldsymbol{u}$ to the second order.

Theorem 3.8 *Let* $(\boldsymbol{u}, 0) \in \boldsymbol{H}_0(\operatorname{curl}, \Omega) \times H_0^1(\Omega)$ *be the solution of the Maxwell equation* (2.8)-(2.9), *and* $(\boldsymbol{u}_h, 0) \in \boldsymbol{V}_h^{c_1} \times V_h^2$ *the solution of the mixed method* (3.5)-(3.6). *Assume* Ω *is convex, then*

$$
\begin{aligned}
\|\boldsymbol{u} - \boldsymbol{u}_h\|_0 &\lesssim \inf_{\boldsymbol{v}_h \in \boldsymbol{V}_h^{c_1}} \left\{ \|\boldsymbol{u} - \boldsymbol{v}_h\|_0 + h\|\operatorname{curl}(\boldsymbol{u} - \boldsymbol{v}_h)\|_0 \right\} \\
&\quad + h\|\operatorname{curl}(\boldsymbol{u} - \boldsymbol{u}_h)\|_0 + \|\boldsymbol{\phi} - \boldsymbol{\phi}_h\|_0,
\end{aligned}
$$

and when $\operatorname{curl} \boldsymbol{w} \in \boldsymbol{H}^1(\Omega; \mathbb{R}^3)$ *and* $\boldsymbol{u} \in \boldsymbol{H}^2(\Omega; \mathbb{R}^3)$,

$$\|\boldsymbol{u} - \boldsymbol{u}_h\|_0 \lesssim h^2(|\operatorname{curl} \boldsymbol{w}|_1 + \|\operatorname{curl} \boldsymbol{u}\|_1 + |\boldsymbol{u}|_2).$$

Proof The proof is adapted from a similar argument in [59] without the data perturbation. Denote $\boldsymbol{e}_h := \boldsymbol{u} - \boldsymbol{u}_h$, then by (2.9) and (3.6), we have $(\boldsymbol{e}_h, \nabla \zeta_h) = 0$ for $\zeta_h \in V_h^2$, thus for any fixed $\boldsymbol{v}_h \in \boldsymbol{V}_h^{c_1}$

$$\|\boldsymbol{e}_h\|_0^2 = (\boldsymbol{e}_h, \boldsymbol{u} - \boldsymbol{v}_h) + (\boldsymbol{e}_h, \boldsymbol{s}_h + \nabla q_h) = (\boldsymbol{e}_h, \boldsymbol{u} - \boldsymbol{v}_h) + (\boldsymbol{e}_h, \boldsymbol{s}_h),$$

where a discrete Helmholtz decomposition

$$\boldsymbol{v}_h - \boldsymbol{u}_h = \boldsymbol{s}_h + \nabla q_h, \quad \text{and } (\boldsymbol{s}_h, \nabla r_h) = 0, \quad \forall r_h \in V_h^2 \tag{3.22}$$

is applied such that $\boldsymbol{s}_h \in \boldsymbol{V}_h^{c_1}$. As a result,

$$\|\boldsymbol{e}_h\|_0 \lesssim \|\boldsymbol{u} - \boldsymbol{v}_h\|_0 + \|\boldsymbol{s}_h\|_0. \tag{3.23}$$

An $H(\text{curl})$-lifting $s \in H_0(\text{curl}, \Omega)$ (see [35, Lemma 7.6, Remark 3.52]) of s_h is sought such that

$$\text{curl } s = \text{curl } s_h, \quad \text{div } s = 0, \quad \text{and} \quad \|s - s_h\|_0 \lesssim h\|\text{curl } s_h\|_0.$$

By the triangle inequality and (3.22),

$$\|s_h\|_0 \leq \|s\|_0 + \|s - s_h\|_0 \lesssim \|s\|_0 + h\|\text{curl } s_h\|_0 = \|s\|_0 + h\|\text{curl}(\boldsymbol{u}_h - \boldsymbol{v}_h)\|_0,$$

hence it suffices to bound $\|s\|_0$. Consequently, the Aubin-Nitsche argument is applied on s, where we seek an $(\boldsymbol{r}, \xi) \in H_0(\text{curl}, \Omega) \times H_0^1(\Omega)$ s.t.

$$(\text{curl } \boldsymbol{r}, \text{curl } \boldsymbol{\chi}) + (\boldsymbol{\chi}, \nabla\xi) = (s, \boldsymbol{\chi}) \quad \forall \boldsymbol{\chi} \in H_0(\text{curl}, \Omega), \tag{3.24}$$

$$(\boldsymbol{r}, \nabla\zeta) = 0 \quad \forall \zeta \in H_0^1(\Omega). \tag{3.25}$$

We have $\xi = 0$ since s is divergence free, and letting $\boldsymbol{\chi} = s$ yields

$$\begin{aligned}
\|s\|_0^2 &= (\text{curl } \boldsymbol{r}, \text{curl } s) = \big(\text{curl } \boldsymbol{r}, \text{curl}(s + \boldsymbol{u}_h - \boldsymbol{v}_h)\big) + \big(\text{curl } \boldsymbol{r}, \text{curl}(-\boldsymbol{u}_h + \boldsymbol{v}_h)\big) \\
&= -\big(\text{curl } \boldsymbol{r}, \text{curl}(\nabla q_h)\big) + \big(\text{curl } \boldsymbol{r}, \text{curl}(\boldsymbol{u} - \boldsymbol{u}_h)\big) - \big(\text{curl } \boldsymbol{r}, \text{curl}(\boldsymbol{u} - \boldsymbol{v}_h)\big).
\end{aligned}$$

By an embedding result (see [24, Chapter 1 Section 3.4]), the Nédélec nodal interpolation $\boldsymbol{I}_h^{c_1}\boldsymbol{r}$ is well-defined, inserting which into the first above, letting $\boldsymbol{\chi} = \boldsymbol{u} - \boldsymbol{v}_h$ in (3.24)–(3.25), and by (3.21), we have

$$\begin{aligned}
\|s\|_0^2 &= \big(\text{curl } \boldsymbol{e}_h, \text{curl}(\boldsymbol{r} - \boldsymbol{I}_h^{c_1}\boldsymbol{r})\big) + (\text{curl } \boldsymbol{e}_h, \text{curl } \boldsymbol{I}_h^{c_1}\boldsymbol{r}) - (s, \boldsymbol{u} - \boldsymbol{v}_h) \\
&= \big(\text{curl } \boldsymbol{e}_h, \text{curl}(\boldsymbol{r} - \boldsymbol{I}_h^{c_1}\boldsymbol{r})\big) + (\boldsymbol{\phi} - \boldsymbol{\phi}_h, \text{curl } \boldsymbol{I}_h^{c_1}\boldsymbol{r}) - (s, \boldsymbol{u} - \boldsymbol{v}_h) \\
&\leq \|\text{curl}(\boldsymbol{r} - \boldsymbol{I}_h^{c_1}\boldsymbol{r})\|_0\|\text{curl } \boldsymbol{e}_h\|_0 + \|\boldsymbol{\phi} - \boldsymbol{\phi}_h\|_0\|\text{curl } \boldsymbol{I}_h^{c_1}\boldsymbol{r}\|_0 + \|s\|_0\|\boldsymbol{u} - \boldsymbol{v}_h\|_0.
\end{aligned}$$

By standard approximation and stability estimates for the nodal interpolation, as well as a regularity estimate for problem (3.24)–(3.25), we have

$$\|\text{curl}(\boldsymbol{r} - \boldsymbol{I}_h^{c_1}\boldsymbol{r})\|_0 \lesssim h|\text{curl } \boldsymbol{r}|_1 \lesssim h\|s\|_0 \quad \text{and} \quad \|\text{curl } \boldsymbol{I}_h^{c_1}\boldsymbol{r}\|_0 \lesssim \|\text{curl } \boldsymbol{r}\|_1 \lesssim \|s\|_0.$$

As a result, we have

$$\|s\|_0 \lesssim h\|\text{curl } \boldsymbol{e}_h\|_0 + \|\boldsymbol{\phi} - \boldsymbol{\phi}_h\|_0 + \|\boldsymbol{u} - \boldsymbol{v}_h\|_0.$$

Lastly, the desired estimate follows from combining the estimates for $\|s_h\|_0$ and $\|s\|_0$ into (3.23). □

3.2 Numerical Verification

In this section, we verify the a priori convergence results shown in the previous subsection. The first example has a smooth solution $\boldsymbol{u}(x, y, z) = \big(0, 0, (\sin x \sin y)^2 \sin z\big)$ on $\Omega = (0, \pi)^3$. Because the true solution is not divergence free, problem (2.9) needs to be modified to $(\boldsymbol{u}, \nabla\zeta) = (g, \zeta)$ with $g = \text{div } \boldsymbol{u}$ being computed from the true solution, and the discretization changes accordingly. The domain Ω is partitioned into a uniform tetrahedral mesh, and the convergence plot is in Fig. 1a. It can be seen that when $\boldsymbol{u}$ and $\text{curl } \boldsymbol{u}$ are smooth, the rates of convergence of $|\boldsymbol{\phi}_I - \boldsymbol{\phi}_h|_{1,h}$ and $\|\boldsymbol{\phi} - \boldsymbol{\phi}_h\|_0$ are optimal, being $O(h)$ and $O(h^2)$, respectively. For the solution u_h obtained from the last Maxwell equation, $\|\text{curl}(\boldsymbol{u} - \boldsymbol{u}_h)\|_0$ is still $O(h)$ and the L^2 error $\|\boldsymbol{u} - \boldsymbol{u}_h\|_0$ is improved to $O(h^2)$.

To demonstrate how the regularity of $\text{curl } \boldsymbol{u}$ which is present in (3.14)–(3.15) shall affect we choose a singular solution on an L-shaped domain (Fig. 2). The true solution is $\boldsymbol{u} =$
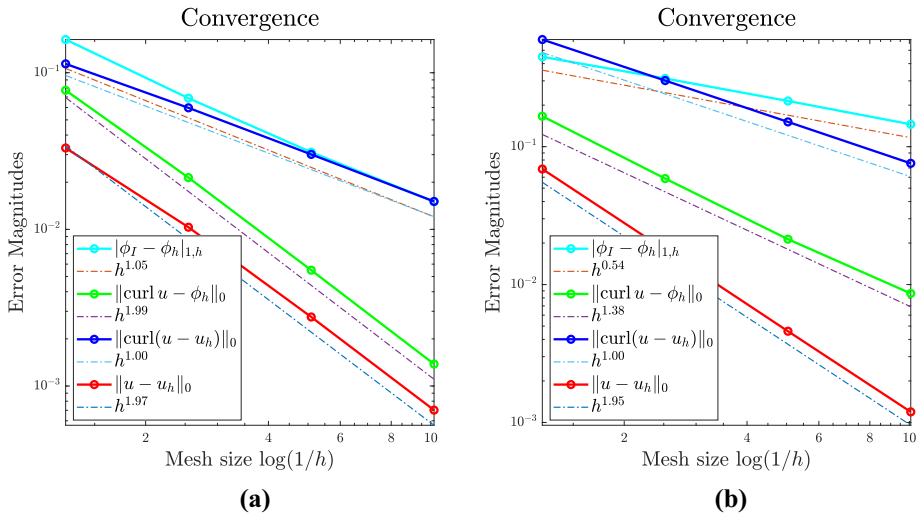
Fig. 1 On a uniformly refined mesh: **a** the convergence of approximating $\boldsymbol{u}(x, y, z) = \left\langle 0, 0, (\sin x \, \sin y)^2 \sin z\right\rangle$. **b** the convergence of approximating $\boldsymbol{u}(x, y, z) = \mathrm{curl}\left\langle 0, 0, r^{8/3}\sin(2\theta/3)\right\rangle$
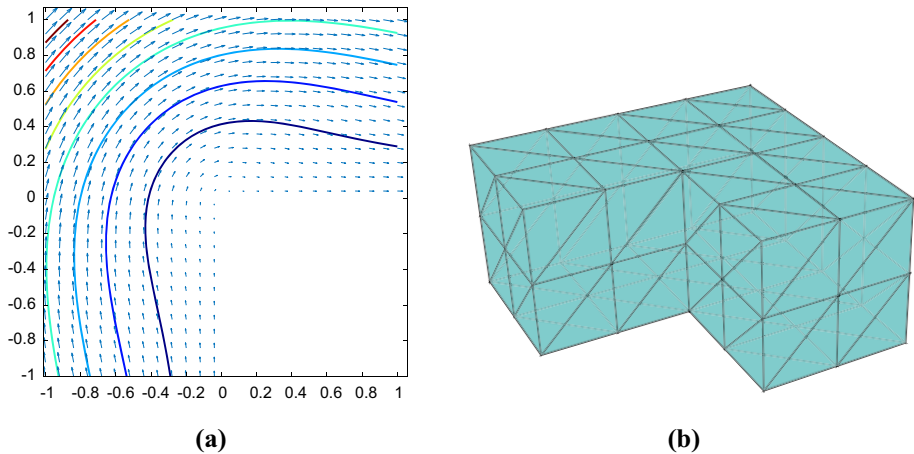
Fig. 2 The true solution vector field shown in (**a**) of the L-shaped domain example viewed from above on $z = 1/4$ plane together with the level set of its z-component. A coarse mesh ($h = 1/2$) can be found in (**b**)

$\mathrm{curl}\langle 0, 0, \mu\rangle$ for a potential function $\mu = r^{8/3}\sin(2\theta/3)$ in the cylindrical coordinate on $\Omega = (1, 1)^2 \times (0, 1/2) \backslash ([0, 1] \times [-1, 0] \times [0, 1/2])$. It can be verified that μ is bi-harmonic so that $\boldsymbol{f} = \boldsymbol{0}$, and $\mathrm{curl}\,\boldsymbol{u} \in \boldsymbol{H}^{5/3-\epsilon}(\Omega; \mathbb{R}^3)$. The convergence of the approximation $\boldsymbol{\phi} = \mathrm{curl}\,\boldsymbol{u}$ in $|\cdot|_{1,h}$ and $\|\cdot\|_0$ are both sub-optimal (Fig. 1b) because $\boldsymbol{\phi} = \mathrm{curl}\,\boldsymbol{u} \notin \boldsymbol{H}^2(\Omega; \mathbb{R}^3)$ which is required to achieve the optimal rate of convergence (see Theorem 3.4 and Remark 3.5). While the approximation for $\boldsymbol{u}$ is optimal as (3.20)'s dependence only on the L^2-error $\|\boldsymbol{\phi} - \boldsymbol{\phi}_h\|_0$ and the approximation property of the linear Nédélec space for $\boldsymbol{u} \in \boldsymbol{H}^{8/3-\epsilon}(\Omega; \mathbb{R}^3)$.

4 A Posteriori Error Analysis

In this section we will propose a reliable and efficient error estimator for the decoupled mixed finite element method (3.1)-(3.4). We aim to get an accurate approximation of $\boldsymbol{u}$ in the energy norm which can be controlled by $\|\operatorname{curl} \boldsymbol{u} - \boldsymbol{\phi}_h\|_0 = \|\boldsymbol{\phi} - \boldsymbol{\phi}_h\|_0 \lesssim |\boldsymbol{\phi} - \boldsymbol{\phi}_h|_{1,h}$. Therefore we do not include problem (3.5)-(3.6) into the adaptive procedure.

To this end, we first recall a quasi-interpolation [16,23,42] and a decomposition of tensor-valued functions [21].

Lemma 4.1 (Theorem 1 in [42]) *There exists an operator* $\boldsymbol{\Pi}_h : \boldsymbol{H}_0(\operatorname{curl}, \Omega) \to \boldsymbol{V}_h^c$ *such that for any* $\boldsymbol{v} \in \boldsymbol{H}_0(\operatorname{curl}, \Omega)$ *there exist* $\tau \in H_0^1(\Omega)$ *and* $\boldsymbol{\chi} \in H_0^1(\Omega; \mathbb{R}^3)$ *satisfying*

$$\boldsymbol{v} - \boldsymbol{\Pi}_h \boldsymbol{v} = \nabla \tau + \boldsymbol{\chi},$$
$$\sum_{K \in \mathcal{T}_h} (h_K^{-2} \|\boldsymbol{\chi}\|_{0,K}^2 + h_K^{-1} \|\boldsymbol{\chi}\|_{0,\partial K}^2) \lesssim \|\operatorname{curl} \boldsymbol{v}\|_0^2. \tag{4.1}$$

Lemma 4.2 (Lemma 3.2 in [21]) *Let* $\boldsymbol{\tau}$ *be a tensor-valued function in* $\boldsymbol{L}^2(\Omega; \mathbb{M})$. *There exist* $\boldsymbol{r} \in \boldsymbol{H}_0^1(\Omega; \mathbb{R}^3)$, $q \in L_0^2(\Omega)$, $\boldsymbol{s} \in \boldsymbol{H}^1(\Omega; \mathbb{M})$ *and* $\boldsymbol{v} \in \boldsymbol{H}_0^2(\Omega; \mathbb{R}^3)$ *such that*

$$\boldsymbol{\tau} = \nabla \boldsymbol{r} - q\boldsymbol{I} + \mathbf{curl}\boldsymbol{s}, \quad \boldsymbol{r} = \operatorname{curl} \boldsymbol{v}, \quad q = \operatorname{tr}(\mathbf{curl}\boldsymbol{s}),$$
$$\|\boldsymbol{r}\|_1 + \|\boldsymbol{s}\|_1 + \|q\|_0 + \|\boldsymbol{v}\|_2 \lesssim \|\boldsymbol{\tau}\|_0.$$

For any subset $\mathcal{M}_h \subseteq \mathcal{T}_h$, define error estimators

$$\eta_1^2(\boldsymbol{w}_h, \boldsymbol{f}, \mathcal{M}_h) := \sum_{K \in \mathcal{M}_h} h_K^2 \|\boldsymbol{f}\|_{0,K}^2 + \sum_{F \in \mathcal{F}_h^i(\mathcal{M}_h)} h_F \|[\![(\operatorname{curl} \boldsymbol{w}_h) \times \boldsymbol{n}_F]\!]\|_{0,F}^2,$$

$$\eta_2^2(\boldsymbol{\phi}_h, \boldsymbol{w}_h, \mathcal{M}_h) := \sum_{K \in \mathcal{M}_h} h_K^2 \|\operatorname{curl} \boldsymbol{w}_h\|_{0,K}^2 + \sum_{F \in \mathcal{F}_h(\mathcal{M}_h)} h_F \|[\![\boldsymbol{n}_F \times (\nabla_h \boldsymbol{\phi}_h)]\!]\|_{0,F}^2.$$

Let $\boldsymbol{Q}_0^K \boldsymbol{f}$ be the $\boldsymbol{L}^2$-projection of the data onto $\prod_{K \in \mathcal{T}_h} \mathbb{P}_0(K; \mathbb{R}^3)$, then the data oscillation is defined as

$$\operatorname{osc}^2(\boldsymbol{f}, \mathcal{M}_h) := \sum_{K \in \mathcal{M}_h} h_K^2 \|\boldsymbol{f} - \boldsymbol{Q}_0^K \boldsymbol{f}\|_{0,K}^2.$$

Let $\boldsymbol{I}_h^{SZ}$ be the tensorial Scott-Zhang interpolation from $\boldsymbol{H}^1(\Omega; \mathbb{M})$ to the tensorial linear Lagrange element space [43]. It holds

$$\sum_{K \in \mathcal{T}_h} \left(h_K^{-2} \|\boldsymbol{v} - \boldsymbol{I}_h^{SZ} \boldsymbol{v}\|_{0,K}^2 + |\boldsymbol{v} - \boldsymbol{I}_h^{SZ} \boldsymbol{v}|_{1,K}^2 \right) \lesssim |\boldsymbol{v}|_1^2 \quad \forall \boldsymbol{v} \in \boldsymbol{H}^1(\Omega; \mathbb{M}). \tag{4.2}$$

We first present the a posteriori error analysis of error $\boldsymbol{w} - \boldsymbol{w}_h$ which is well-documented for the saddle point formulation of Maxwell's equation (see e.g., [4,56,58]). We include a proof here for the completeness.

Lemma 4.3 *Let* $(\boldsymbol{w}, 0) \in \boldsymbol{H}_0(\operatorname{curl}, \Omega) \times H_0^1(\Omega)$ *be the solution of the Maxwell equation* (2.4)-(2.5), *and* $(\boldsymbol{w}_h, 0) \in \boldsymbol{V}_h^c \times V_h^1$ *the solution of the mixed method* (3.1)–(3.2). *We have*

$$\|\operatorname{curl}(\boldsymbol{w} - \boldsymbol{w}_h)\|_0 \lesssim \eta_1(\boldsymbol{w}_h, \boldsymbol{f}, \mathcal{T}_h), \tag{4.3}$$
$$\eta_1(\boldsymbol{w}_h, \boldsymbol{f}, \mathcal{T}_h) \lesssim \|\operatorname{curl}(\boldsymbol{w} - \boldsymbol{w}_h)\|_0 + \operatorname{osc}(\boldsymbol{f}, \mathcal{T}_h). \tag{4.4}$$

Proof Applying Lemma 4.1 to $\boldsymbol{v} = \boldsymbol{w} - \boldsymbol{w}_h$, we get from (3.7) and (2.4) that

$$
\begin{aligned}
\|\operatorname{curl}(\boldsymbol{w} - \boldsymbol{w}_h)\|_0^2 &= (\operatorname{curl}(\boldsymbol{w} - \boldsymbol{w}_h), \operatorname{curl}(\boldsymbol{v} - \boldsymbol{\Pi}_h \boldsymbol{v})) = (\operatorname{curl}(\boldsymbol{w} - \boldsymbol{w}_h), \operatorname{curl}\boldsymbol{\chi}) \\
&= (\boldsymbol{f}, \boldsymbol{\chi}) - (\operatorname{curl}\boldsymbol{w}_h, \operatorname{curl}\boldsymbol{\chi}) \\
&= (\boldsymbol{f}, \boldsymbol{\chi}) - \sum_{K \in \mathcal{T}_h} ((\operatorname{curl}\boldsymbol{w}_h) \times \boldsymbol{n}, \boldsymbol{\chi})_{\partial K} \\
&= (\boldsymbol{f}, \boldsymbol{\chi}) - \sum_{F \in \mathcal{F}_h^i} (\llbracket (\operatorname{curl}\boldsymbol{w}_h) \times \boldsymbol{n}_F \rrbracket, \boldsymbol{\chi})_F.
\end{aligned}
$$

Hence we have derived (4.3) by (4.1).

The efficiency (4.4) follows from the standard bubble function techniques (see e.g., [4]).

$\square$

Lemma 4.4 *Let* $(\boldsymbol{w}, 0, \boldsymbol{\phi}, p) \in \boldsymbol{H}_0(\operatorname{curl}, \Omega) \times H_0^1(\Omega) \times \boldsymbol{H}_0^1(\Omega; \mathbb{R}^3) \times L_0^2(\Omega)$ *be the solution of the variational formulation* (2.4)–(2.7), *and* $(\boldsymbol{w}_h, 0, \boldsymbol{\phi}_h, p_h) \in \boldsymbol{V}_h^c \times V_h^1 \times \boldsymbol{V}_h^{CR} \times \mathcal{Q}_h$ *the solution of the mixed method* (3.1)–(3.4). *We have*

$$
|\boldsymbol{\phi} - \boldsymbol{\phi}_h|_{1,h} + h\|\operatorname{curl}(\boldsymbol{w} - \boldsymbol{w}_h)\|_0 \lesssim h\eta_1(\boldsymbol{w}_h, \boldsymbol{f}, \mathcal{T}_h) + \eta_2(\boldsymbol{\phi}_h, \boldsymbol{w}_h, \mathcal{T}_h), \tag{4.5}
$$

$$
h\eta_1(\boldsymbol{w}_h, \boldsymbol{f}, \mathcal{T}_h) + \eta_2(\boldsymbol{\phi}_h, \boldsymbol{w}_h, \mathcal{T}_h) \lesssim |\boldsymbol{\phi} - \boldsymbol{\phi}_h|_{1,h} + \|p - p_h\|_0 \\
+ h\|\operatorname{curl}(\boldsymbol{w} - \boldsymbol{w}_h)\|_0 + h\operatorname{osc}(\boldsymbol{f}, \mathcal{T}_h). \tag{4.6}
$$

Proof Applying Lemma 4.2 to $\nabla_h(\boldsymbol{\phi} - \boldsymbol{\phi}_h)$, there exist $\boldsymbol{r} \in \boldsymbol{H}_0^1(\Omega; \mathbb{R}^3)$, $q \in L_0^2(\Omega)$, $\boldsymbol{s} \in \boldsymbol{H}^1(\Omega; \mathbb{M})$ and $\boldsymbol{v} \in \boldsymbol{H}_0^2(\Omega; \mathbb{R}^3)$ such that

$$
\nabla_h(\boldsymbol{\phi} - \boldsymbol{\phi}_h) = \nabla \boldsymbol{r} - q\boldsymbol{I} + \operatorname{curl}\boldsymbol{s}, \quad \boldsymbol{r} = \operatorname{curl}\boldsymbol{v},
$$
$$
\|\boldsymbol{r}\|_1 + \|\boldsymbol{s}\|_1 + \|q\|_0 + \|\boldsymbol{v}\|_2 \lesssim \|\nabla_h(\boldsymbol{\phi} - \boldsymbol{\phi}_h)\|_0. \tag{4.7}
$$

Note that $\operatorname{div}_h(\boldsymbol{\phi} - \boldsymbol{\phi}_h) = 0$ from (2.7) and (3.4). Since $\operatorname{div}\boldsymbol{r} = 0$, we get from (2.6) that

$$
\begin{aligned}
|\boldsymbol{\phi} - \boldsymbol{\phi}_h|_{1,h}^2 &= (\nabla_h(\boldsymbol{\phi} - \boldsymbol{\phi}_h), \nabla \boldsymbol{r} - q\boldsymbol{I} + \operatorname{curl}\boldsymbol{s}) = (\nabla_h(\boldsymbol{\phi} - \boldsymbol{\phi}_h), \nabla \boldsymbol{r} + \operatorname{curl}\boldsymbol{s}) \\
&= (\nabla_h(\boldsymbol{\phi} - \boldsymbol{\phi}_h), \nabla \boldsymbol{r}) + (\operatorname{div}\boldsymbol{r}, p - p_h) + (\nabla_h(\boldsymbol{\phi} - \boldsymbol{\phi}_h), \operatorname{curl}\boldsymbol{s}) \\
&= (\operatorname{curl}\boldsymbol{w}, \boldsymbol{r}) - (\nabla_h\boldsymbol{\phi}_h, \nabla \boldsymbol{r}) - (\operatorname{div}\boldsymbol{r}, p_h) - (\nabla_h\boldsymbol{\phi}_h, \operatorname{curl}\boldsymbol{s}).
\end{aligned}
$$

It follows from (3.9) and (3.3) that

$$
(\nabla_h\boldsymbol{\phi}_h, \nabla \boldsymbol{r}) + (\operatorname{div}\boldsymbol{r}, p_h) = (\nabla_h\boldsymbol{\phi}_h, \nabla(I_h^s \boldsymbol{r})) + (\operatorname{div}(I_h^s \boldsymbol{r}), p_h) = (\operatorname{curl}\boldsymbol{w}_h, I_h^s \boldsymbol{r}).
$$

Noticing that $(\nabla_h\boldsymbol{\phi}_h, \operatorname{curl}(I_h^{SZ}\boldsymbol{s})) = 0$, we obtain from the last two identities that

$$
\begin{aligned}
|\boldsymbol{\phi} - \boldsymbol{\phi}_h|_{1,h}^2 &= (\operatorname{curl}\boldsymbol{w}, \boldsymbol{r}) - (\operatorname{curl}\boldsymbol{w}_h, I_h^s \boldsymbol{r}) - (\nabla_h\boldsymbol{\phi}_h, \operatorname{curl}(\boldsymbol{s} - I_h^{SZ}\boldsymbol{s})) \\
&= (\operatorname{curl}(\boldsymbol{w} - \boldsymbol{w}_h), \operatorname{curl}\boldsymbol{v}) + (\operatorname{curl}\boldsymbol{w}_h, \boldsymbol{r} - I_h^s \boldsymbol{r}) \\
&\quad - (\nabla_h\boldsymbol{\phi}_h, \operatorname{curl}(\boldsymbol{s} - I_h^{SZ}\boldsymbol{s})). \tag{4.8}
\end{aligned}
$$

Next we estimate the right hand side of (4.8) term by term. Employing (3.7) and (4.3), it follows

$$
\begin{aligned}
(\operatorname{curl}(\boldsymbol{w} - \boldsymbol{w}_h), \operatorname{curl}\boldsymbol{v}) &= \inf_{\boldsymbol{v}_h \in \boldsymbol{V}_h^c} (\operatorname{curl}(\boldsymbol{w} - \boldsymbol{w}_h), \operatorname{curl}(\boldsymbol{v} - \boldsymbol{v}_h)) \\
&\leq \|\operatorname{curl}(\boldsymbol{w} - \boldsymbol{w}_h)\|_0 \inf_{\boldsymbol{v}_h \in \boldsymbol{V}_h^c} \|\operatorname{curl}(\boldsymbol{v} - \boldsymbol{v}_h)\|_0 \\
&\lesssim h\eta_1(\boldsymbol{w}_h, \boldsymbol{f}, \mathcal{T}_h)|\operatorname{curl}\boldsymbol{v}|_1 = h\eta_1(\boldsymbol{w}_h, \boldsymbol{f}, \mathcal{T}_h)|\boldsymbol{r}|_1.
\end{aligned}
$$

According to (3.10), we have

$$(\operatorname{curl} \boldsymbol{w}_h, \boldsymbol{r} - \boldsymbol{I}_h^s \boldsymbol{r}) \lesssim \eta_2(\boldsymbol{\phi}_h, \boldsymbol{w}_h, \mathcal{T}_h)|\boldsymbol{r}|_1.$$

And we get from (4.2) that

$$
\begin{aligned}
-(\nabla_h \boldsymbol{\phi}_h, \mathbf{curl}(\boldsymbol{s} - \boldsymbol{I}_h^{SZ} \boldsymbol{s})) &= \sum_{K \in \mathcal{T}_h} (\boldsymbol{n} \times (\nabla_h \boldsymbol{\phi}_h), \boldsymbol{s} - \boldsymbol{I}_h^{SZ} \boldsymbol{s})_{\partial K} \\
&= \sum_{F \in \mathcal{F}_h} (\llbracket \boldsymbol{n}_F \times (\nabla_h \boldsymbol{\phi}_h) \rrbracket, \boldsymbol{s} - \boldsymbol{I}_h^{SZ} \boldsymbol{s})_F \\
&\lesssim \eta_2(\boldsymbol{\phi}_h, \boldsymbol{w}_h, \mathcal{T}_h)|\boldsymbol{s}|_1.
\end{aligned}
$$

Combining the last three inequalities and (4.8), we get from (4.7) that

$$|\boldsymbol{\phi} - \boldsymbol{\phi}_h|_{1,h} \lesssim h\eta_1(\boldsymbol{w}_h, \boldsymbol{f}, \mathcal{T}_h) + \eta_2(\boldsymbol{\phi}_h, \boldsymbol{w}_h, \mathcal{T}_h),$$

which together with (4.3) indicates (4.5).

On the other side, by applying the bubble function techniques, we get

$$\sum_{K \in \mathcal{T}_h} h_K^2 \|\operatorname{curl} \boldsymbol{w}_h\|_{0,K}^2 \lesssim h^2 \|\operatorname{curl}(\boldsymbol{w} - \boldsymbol{w}_h)\|_0^2 + |\boldsymbol{\phi} - \boldsymbol{\phi}_h|_{1,h}^2 + \|p - p_h\|_0^2,$$

$$\sum_{F \in \mathcal{F}_h} h_F \|\llbracket \boldsymbol{n}_F \times (\nabla_h \boldsymbol{\phi}_h) \rrbracket\|_{0,F}^2 \lesssim |\boldsymbol{\phi} - \boldsymbol{\phi}_h|_{1,h}^2.$$

Combining the last two inequalities shows

$$\eta_2(\boldsymbol{\phi}_h, \boldsymbol{w}_h, \mathcal{T}_h) \lesssim h\|\operatorname{curl}(\boldsymbol{w} - \boldsymbol{w}_h)\|_0 + |\boldsymbol{\phi} - \boldsymbol{\phi}_h|_{1,h} + \|p - p_h\|_0.$$

Therefore we conclude (4.6) from (4.4). □

By the a priori L^2-estimate of the Stokes problem, when we assume the H^{1+s}-regularity ($s \in (1/2, 1]$) for the possible non-smooth solution, the following estimate, combining with Lemmas 4.3 and 4.4, can be used for a global reliability bound for $\|\boldsymbol{\phi} - \boldsymbol{\phi}_h\|_0$.

Lemma 4.5 *Let* $(\boldsymbol{w}, 0, \boldsymbol{\phi}, p) \in \boldsymbol{H}_0(\operatorname{curl}, \Omega) \times H_0^1(\Omega) \times \boldsymbol{H}_0^1(\Omega; \mathbb{R}^3) \times L_0^2(\Omega)$ *be the solution of the variational formulation* (2.4)–(2.7), *and* $(\boldsymbol{w}_h, 0, \boldsymbol{\phi}_h, p_h) \in \boldsymbol{V}_h^c \times V_h^1 \times \boldsymbol{V}_h^{CR} \times \mathcal{Q}_h$ *the solution of the mixed method* (3.1)–(3.4). *We have*

$$\|\boldsymbol{\phi} - \boldsymbol{\phi}_h\|_0 \lesssim h^s |\boldsymbol{\phi} - \boldsymbol{\phi}_h|_{1,h} + h\|\operatorname{curl}(\boldsymbol{w} - \boldsymbol{w}_h)\|_0 + h^{1+s}\|\operatorname{curl} \boldsymbol{w}_h\|_0.$$

5 Quasi-orthogonality

In this section we will develop the quasi-orthogonality of the decoupled mixed finite element method.

5.1 Discrete Complexes in Three Dimensions

First recall a nonconforming discretization of the following Stokes complex in three dimensions [30]

$$0 \longrightarrow H_0^1(\Omega) \xrightarrow{\nabla} \boldsymbol{H}_0(\operatorname{grad} \operatorname{curl}, \Omega) \xrightarrow{\operatorname{curl}} \boldsymbol{H}_0^1(\Omega; \mathbb{R}^3) \xrightarrow{\operatorname{div}} L_0^2(\Omega) \longrightarrow 0,$$

where $\boldsymbol{H}_0(\text{grad curl}, \Omega) := \{\boldsymbol{v} \in \boldsymbol{H}_0(\text{curl}, \Omega) : \text{curl}\,\boldsymbol{v} \in \boldsymbol{H}_0^1(\Omega; \mathbb{R}^3)\}$. Note that $\boldsymbol{H}_0(\text{grad curl}, \Omega) = \boldsymbol{H}_0(\text{curl curl}, \Omega)$ in (2.3) (cf. [53]).

The space of the shape functions of the $\boldsymbol{H}(\text{grad curl})$ nonconforming element proposed in [30] is $\mathbb{P}_0(K; \mathbb{R}^3) \oplus \boldsymbol{x} \wedge \mathbb{P}_1(K; \mathbb{R}^3)$, and the local degrees of freedom are given by

$$\int_e \boldsymbol{v} \cdot \boldsymbol{t}_e \, \mathrm{d}s \quad \text{on each } e \in \mathcal{E}(K), \tag{5.1}$$

$$\int_F (\text{curl}\,\boldsymbol{v}) \cdot \boldsymbol{t}_{F,i} \, \mathrm{d}s \quad \text{on each } F \in \mathcal{F}(K) \text{ with } i = 1, 2. \tag{5.2}$$

The global $\boldsymbol{H}(\text{grad curl})$ nonconforming element space is then defined as

$$\boldsymbol{W}_h := \{\boldsymbol{v}_h \in \boldsymbol{L}^2(\Omega; \mathbb{R}^3) : \boldsymbol{v}_h|_K \in \mathbb{P}_0(K; \mathbb{R}^3) \oplus \boldsymbol{x} \wedge \mathbb{P}_1(K; \mathbb{R}^3) \text{ for each } K \in \mathcal{T}_h,$$

$$\text{all the degree of freedom } (5.1)-(5.2) \text{ are single-valued,}$$

$$\text{and all the degree of freedom } (5.1)-(5.2) \text{ on } \partial\Omega \text{ vanish}\}.$$

Now the nonconforming discrete Stokes complex in [30] is presented as

$$0 \longrightarrow V_h^1 \xrightarrow{\nabla} \boldsymbol{W}_h \xrightarrow{\text{curl}_h} V_h^{\text{CR}} \xrightarrow{\text{div}_h} \mathcal{Q}_h \longrightarrow 0. \tag{5.3}$$

We also need the help of a discrete de Rham complex. Recall the lowest-order Raviart-Thomas element space [37,41]

$$\boldsymbol{V}_h^d := \{\boldsymbol{v}_h \in \boldsymbol{H}_0(\text{div}, \Omega) : \boldsymbol{v}_h|_K \in \mathbb{P}_0(K; \mathbb{R}^3) + \boldsymbol{x}\mathbb{P}_0(K) \text{ for each } K \in \mathcal{T}_h\},$$

and the discrete de Rham complex [1,2]

$$0 \longrightarrow V_h^1 \xrightarrow{\nabla} \boldsymbol{V}_h^c \xrightarrow{\text{curl}} \boldsymbol{V}_h^d \xrightarrow{\text{div}} \mathcal{Q}_h \longrightarrow 0.$$

Let $\boldsymbol{I}_h^c$ be the nodal interpolation operator from $\text{Dom}(\boldsymbol{I}_h^c)$ to $\boldsymbol{V}_h^c$, and $\boldsymbol{I}_h^d$ the nodal interpolation operator from $\text{Dom}(\boldsymbol{I}_h^d)$ to $\boldsymbol{V}_h^d$, where $\text{Dom}(\boldsymbol{I}_h^c)$ and $\text{Dom}(\boldsymbol{I}_h^d)$ are the domains of the operators $\boldsymbol{I}_h^c$ and $\boldsymbol{I}_h^d$ respectively. It holds for any $\boldsymbol{v}_h \in \boldsymbol{W}_h$ that

$$\|\text{curl}_h(\boldsymbol{v}_h - \boldsymbol{I}_h^c \boldsymbol{v}_h)\|_{0,K} = \|\text{curl}_h \boldsymbol{v}_h - \boldsymbol{I}_h^d(\text{curl}_h \boldsymbol{v}_h)\|_{0,K} \lesssim h_K |\text{curl}_h \boldsymbol{v}_h|_{1,K}.$$

Henceforth, consider two nested conforming triangulations $\mathcal{T}_h$ and $\mathcal{T}_H$, where $\mathcal{T}_h$ is a refinement of $\mathcal{T}_H$. We have the commutative diagram property [1,2]

$$\text{curl}(\boldsymbol{I}_H^c \boldsymbol{v}_h) = \boldsymbol{I}_H^d(\text{curl}_h \boldsymbol{v}_h) \quad \forall \boldsymbol{v}_h \in \boldsymbol{V}_h^c + \boldsymbol{W}_h. \tag{5.4}$$

To derive the quasi-orthogonality, we need the following interpolation error estimation for $\boldsymbol{I}_H^s$ [26]

$$\|\boldsymbol{\psi}_h - \boldsymbol{I}_H^s \boldsymbol{\psi}_h\|_{0,K} \lesssim h_K \|\nabla_h \boldsymbol{\psi}_h\|_{0,K} \quad \forall \boldsymbol{\psi}_h \in \boldsymbol{V}_h^{\text{CR}}, K \in \mathcal{T}_H \backslash \mathcal{T}_h. \tag{5.5}$$

According to (3.1), since the triangulations $\mathcal{T}_h$ and $\mathcal{T}_H$ are nested, we get the following Galerkin orthogonality

$$(\text{curl}(\boldsymbol{w}_h - \boldsymbol{w}_H), \text{curl}\,\boldsymbol{v}_H) = 0 \quad \forall \boldsymbol{v}_H \in \boldsymbol{V}_H^c. \tag{5.6}$$

Lemma 5.1 *It holds*

$$\sum_{K \in \mathcal{T}_H} h_K^{-2} \|\boldsymbol{\psi}_h - \boldsymbol{I}_H^d \boldsymbol{\psi}_h\|_{0,K}^2 \lesssim |\boldsymbol{\psi}_h|_{1,h}^2 \quad \forall \boldsymbol{\psi}_h \in \boldsymbol{V}_h^{\text{CR}}. \tag{5.7}$$

Proof By the averaging technique [7,29], there exists $\widetilde{\boldsymbol{\psi}}_h \in \boldsymbol{V}_h^1 := V_h^1 \otimes \mathbb{R}^3$ such that

$$|\widetilde{\boldsymbol{\psi}}_h|_1^2 + \sum_{K \in \mathcal{T}_h} \left(h_K^{-2} \|\boldsymbol{\psi}_h - \widetilde{\boldsymbol{\psi}}_h\|_{0,K}^2 + h_K^{-1} \|\boldsymbol{\psi}_h - \widetilde{\boldsymbol{\psi}}_h\|_{0,\partial K}^2 \right) \lesssim |\boldsymbol{\psi}_h|_{1,h}^2. \tag{5.8}$$

Applying the scaling argument, we get

$$\sum_{K \in \mathcal{T}_H} h_K^{-2} \|\boldsymbol{I}_H^d(\boldsymbol{\psi}_h - \widetilde{\boldsymbol{\psi}}_h)\|_{0,K}^2 \lesssim \sum_{K \in \mathcal{T}_H} h_K^{-1} \|(\boldsymbol{\psi}_h - \widetilde{\boldsymbol{\psi}}_h) \cdot \boldsymbol{n}\|_{0,\partial K}^2$$

$$\leq \sum_{K \in \mathcal{T}_H} h_K^{-1} \left(\sum_{K' \in \mathcal{T}_h(K)} \|\boldsymbol{\psi}_h - \widetilde{\boldsymbol{\psi}}_h\|_{0,\partial K'}^2 \right)$$

$$\leq \sum_{K \in \mathcal{T}_h} h_K^{-1} \|\boldsymbol{\psi}_h - \widetilde{\boldsymbol{\psi}}_h\|_{0,\partial K}^2.$$

Noting that $\widetilde{\boldsymbol{\psi}}_h \in \boldsymbol{H}_0^1(\Omega; \mathbb{R}^3)$, it follows

$$\sum_{K \in \mathcal{T}_H} h_K^{-2} \|\widetilde{\boldsymbol{\psi}}_h - \boldsymbol{I}_H^d \widetilde{\boldsymbol{\psi}}_h\|_{0,K}^2 \lesssim |\widetilde{\boldsymbol{\psi}}_h|_{1,h}^2.$$

Combining the last two inequalities and (5.8) yields

$$\sum_{K \in \mathcal{T}_H} h_K^{-2} \left(\|\boldsymbol{I}_H^d(\boldsymbol{\psi}_h - \widetilde{\boldsymbol{\psi}}_h)\|_{0,K}^2 + \|\boldsymbol{\psi}_h - \widetilde{\boldsymbol{\psi}}_h\|_{0,K}^2 + \|\widetilde{\boldsymbol{\psi}}_h - \boldsymbol{I}_H^d \widetilde{\boldsymbol{\psi}}_h\|_{0,K}^2 \right) \lesssim |\boldsymbol{\psi}_h|_{1,h}^2.$$

On the other hand, we have

$$\|\boldsymbol{\psi}_h - \boldsymbol{I}_H^d \boldsymbol{\psi}_h\|_{0,K} \leq \|\boldsymbol{I}_H^d(\boldsymbol{\psi}_h - \widetilde{\boldsymbol{\psi}}_h)\|_{0,K} + \|\boldsymbol{\psi}_h - \widetilde{\boldsymbol{\psi}}_h\|_{0,K} + \|\widetilde{\boldsymbol{\psi}}_h - \boldsymbol{I}_H^d \widetilde{\boldsymbol{\psi}}_h\|_{0,K}.$$

Therefore we conclude (5.7) from the last two inequalities. □

5.2 Quasi-orthogonality

Lemma 5.2 (quasi-orthogonality of $\boldsymbol{\phi}$) *Let* $(\boldsymbol{w}_h, 0, \boldsymbol{\phi}_h, p_h) \in \boldsymbol{V}_h^c \times V_h^1 \times \boldsymbol{V}_h^{\mathrm{CR}} \times \mathcal{Q}_h$ *and* $(\boldsymbol{w}_H, 0, \boldsymbol{\phi}_H, p_H) \in \boldsymbol{V}_H^c \times V_h^1 \times \boldsymbol{V}_h^{\mathrm{CR}} \times \mathcal{Q}_H$ *the solutions of the mixed method* (3.1)-(3.4) *on triangulations* $\mathcal{T}_h$ *and* $\mathcal{T}_H$ *respectively. We have*

$$(\nabla_h(\boldsymbol{\phi} - \boldsymbol{\phi}_h), \nabla_h(\boldsymbol{\phi}_h - \boldsymbol{\phi}_H)) \lesssim H|\boldsymbol{\phi} - \boldsymbol{\phi}_h|_{1,h} \|\operatorname{curl}(\boldsymbol{w}_h - \boldsymbol{w}_H)\|_0$$

$$+ |\boldsymbol{\phi} - \boldsymbol{\phi}_h|_{1,h} \left(\sum_{K \in \mathcal{T}_H \setminus \mathcal{T}_h} h_K^2 \|\operatorname{curl} \boldsymbol{w}_H\|_{0,K}^2 \right)^{1/2}. \tag{5.9}$$

Proof Let $\boldsymbol{\psi}_h = \boldsymbol{I}_h^s(\boldsymbol{\phi} - \boldsymbol{\phi}_h)$, then we get from (3.9) and (3.10) that

$$\operatorname{div}_h \boldsymbol{\psi}_h = 0, \quad |\boldsymbol{\psi}_h|_{1,h} \lesssim |\boldsymbol{\phi} - \boldsymbol{\phi}_h|_{1,h}. \tag{5.10}$$

It follows from (3.4), (3.9) and (3.3) that

$$(\nabla_h(\boldsymbol{\phi} - \boldsymbol{\phi}_h), \nabla_h(\boldsymbol{\phi}_h - \boldsymbol{\phi}_H)) = (\nabla_h(\boldsymbol{\phi} - \boldsymbol{\phi}_h), \nabla_h \boldsymbol{\phi}_h + p_h \boldsymbol{I} - (\nabla_H \boldsymbol{\phi}_H + p_H \boldsymbol{I}))$$

$$= (\nabla_h \boldsymbol{\phi}_h + p_h \boldsymbol{I} - (\nabla_H \boldsymbol{\phi}_H + p_H \boldsymbol{I}), \nabla_h \boldsymbol{\psi}_h)$$

$$= (\operatorname{curl} \boldsymbol{w}_h, \boldsymbol{\psi}_h) - (\nabla_H \boldsymbol{\phi}_H + p_H \boldsymbol{I}, \nabla_h \boldsymbol{\psi}_h)$$

$$= (\operatorname{curl} \boldsymbol{w}_h, \boldsymbol{\psi}_h) - (\nabla_H \boldsymbol{\phi}_H + p_H \boldsymbol{I}, \nabla_h(\boldsymbol{I}_H^s \boldsymbol{\psi}_h))$$

$$= (\operatorname{curl} \boldsymbol{w}_h, \boldsymbol{\psi}_h) - (\operatorname{curl} \boldsymbol{w}_H, \boldsymbol{I}_H^s \boldsymbol{\psi}_h).$$

Thus we have

$$(\nabla_h(\boldsymbol{\phi} - \boldsymbol{\phi}_h), \nabla_h(\boldsymbol{\phi}_h - \boldsymbol{\phi}_H)) = (\text{curl}(\boldsymbol{w}_h - \boldsymbol{w}_H), \boldsymbol{\psi}_h)$$
$$+ (\text{curl }\boldsymbol{w}_H, \boldsymbol{\psi}_h - \boldsymbol{I}_H^s \boldsymbol{\psi}_h). \qquad (5.11)$$

Next we estimate the right hand side of the last equation term by term.

Due to the discrete Stokes complex (5.3) and the fact $\text{div}_h \boldsymbol{\psi}_h = 0$, there exists $\boldsymbol{v}_h \in \boldsymbol{W}_h$ such that $\boldsymbol{\psi}_h = \text{curl}_h \boldsymbol{v}_h$. From (5.6) and (5.4), we have

$$\begin{aligned}
(\text{curl}(\boldsymbol{w}_h - \boldsymbol{w}_H), \boldsymbol{\psi}_h) &= (\text{curl}(\boldsymbol{w}_h - \boldsymbol{w}_H), \text{curl}_h \boldsymbol{v}_h) \\
&= (\text{curl}(\boldsymbol{w}_h - \boldsymbol{w}_H), \text{curl}_h(\boldsymbol{v}_h - \boldsymbol{I}_H^c \boldsymbol{v}_h)) \\
&= (\text{curl}(\boldsymbol{w}_h - \boldsymbol{w}_H), \text{curl}_h \boldsymbol{v}_h - \boldsymbol{I}_H^d \text{curl}_h \boldsymbol{v}_h) \\
&= (\text{curl}(\boldsymbol{w}_h - \boldsymbol{w}_H), \boldsymbol{\psi}_h - \boldsymbol{I}_H^d \boldsymbol{\psi}_h).
\end{aligned}$$

Then it holds from (5.7) that

$$(\text{curl}(\boldsymbol{w}_h - \boldsymbol{w}_H), \boldsymbol{\psi}_h) \lesssim H \| \text{curl}(\boldsymbol{w}_h - \boldsymbol{w}_H) \|_0 |\boldsymbol{\psi}_h|_{1,h}.$$

Thanks to (5.5), we obtain

$$\begin{aligned}
(\text{curl }\boldsymbol{w}_H, \boldsymbol{\psi}_h - \boldsymbol{I}_H^s \boldsymbol{\psi}_h) &= \sum_{K \in \mathcal{T}_H \backslash \mathcal{T}_h} (\text{curl }\boldsymbol{w}_H, \boldsymbol{\psi}_h - \boldsymbol{I}_H^s \boldsymbol{\psi}_h)_K \\
&\lesssim |\boldsymbol{\psi}_h|_{1,h} \left(\sum_{K \in \mathcal{T}_H \backslash \mathcal{T}_h} h_K^2 \| \text{curl }\boldsymbol{w}_H \|_{0,K}^2 \right)^{1/2}.
\end{aligned}$$

Finally we conclude from (5.11), the last two inequalities and (5.10). $\qquad\square$

6 Convergence

In this section, we propose an adaptive algorithm (Algorithm 1) based on the estimators in Sect. 4. Then its convergence is proved using the quasi-orthogonality in Sect. 5. The methodology in the convergence mainly follows that of [26]. There are two major modifications: one first needs to control the perturbation of data for the Stokes problem, then the convergence is proved only for $\| \text{curl}(\boldsymbol{u} - \boldsymbol{u}_h) \|_0$ and $|\boldsymbol{\phi} - \boldsymbol{\phi}_h|_{1,h}$ without the Lagrange multiplier variable. Notice that if conforming stable Stokes pairs are used, the convergence of any adaptive finite element method for Stokes equation is extremely hard as the velocity and the pressure are coupled together.

For the ease of the readers, the following short notations are adopted throughout the proof of the contraction in Theorem 6.3 and the lemmas needed. For $\boldsymbol{V}_h$ defined on $\mathcal{T}_k$, we denote them by $\boldsymbol{V}_k^c$ and $\boldsymbol{V}_k^{\text{CR}}$. Similarly, the approximations on $\mathcal{T}_k$ are denoted by $\boldsymbol{w}_k, \boldsymbol{\phi}_k$, and $\boldsymbol{u}_k$ respectively. Let $h_k := \max_{K \in \mathcal{T}_k} h_K$, and denote the quantities involving two consecutive levels of meshes as follows:

$$E_k := |\boldsymbol{\phi} - \boldsymbol{\phi}_k|_{1,k} := \left(\sum_{K \in \mathcal{T}_k} \| \nabla_k(\boldsymbol{\phi} - \boldsymbol{\phi}_k) \|_{0,K}^2 \right)^{1/2},$$

$$R_{k+1} := |\boldsymbol{\phi}_k - \boldsymbol{\phi}_{k+1}|_{1,k+1} := \left(\sum_{K \in \mathcal{T}_{k+1}} \| \nabla_{k+1}(\boldsymbol{\phi}_k - \boldsymbol{\phi}_{k+1}) \|_{0,K}^2 \right)^{1/2},$$

$$e_k := \| \operatorname{curl}(\boldsymbol{w} - \boldsymbol{w}_k) \|_0, \quad r_{k+1} := \| \operatorname{curl}(\boldsymbol{w}_k - \boldsymbol{w}_{k+1}) \|_0,$$

$$\eta_{1,k}(\mathcal{M}) := \eta_1(\boldsymbol{w}_k, \boldsymbol{f}, \mathcal{M}),$$

$$\eta_{2,k}(\mathcal{M}) := \eta_2(\boldsymbol{\phi}_k, \boldsymbol{w}_k, \mathcal{M}),$$

$$g_k(\mathcal{M}) := \left(\sum_{K \in \mathcal{M}} h_K^2 \| \operatorname{curl} \boldsymbol{w}_k \|_{0,K}^2 \right)^{1/2},$$

where ∇_k stands for the discrete gradient ∇_h defined piecewisely on all $K \in \mathcal{T}_k$, and $\mathcal{M}$ can be $\mathcal{T}_k$, $\mathcal{T}_{k+1}$, or $\mathcal{T}_k \setminus \mathcal{T}_{k+1}$.

Algorithm 1 An adaptive nonconforming finite element method

Input: $\mathcal{T}_0, \boldsymbol{f}, \texttt{tol}, \theta_1, \theta_2 \in (0, 1)$.
Output: $\mathcal{T}_N, \boldsymbol{\phi}_N, \boldsymbol{u}_N$.
1: $\eta_1 = \texttt{tol}, \eta_2 = \texttt{tol}, k = 0$.
2: **while** True **do**
3:     **SOLVE**: Solve (3.1)–(3.2) and (3.3)–(3.4) on $\mathcal{T}_k$ to get $(\boldsymbol{w}_k, \boldsymbol{\phi}_k)$;
4:     **ESTIMATE**: Compute $\eta_1(\boldsymbol{w}_k, \boldsymbol{f}, K)$ and $\eta_2(\boldsymbol{\phi}_k, \boldsymbol{w}_k, K)$ for all $K \in \mathcal{T}_k$
5:          $\eta_1 \leftarrow \eta_1(\boldsymbol{w}_k, \boldsymbol{f}, \mathcal{T}_k)$
6:          $\eta_2 \leftarrow \eta_2(\boldsymbol{\phi}_k, \boldsymbol{w}_k, \mathcal{T}_k)$
7:     **if** $\eta_1 < \texttt{tol}$ and $\eta_2 < \texttt{tol}$ **then**
8:         Break
9:     **end if**
10:    **MARK**: Seek a minimum $\mathcal{M} \subseteq \mathcal{T}_k$ such that

$$\eta_1^2(\boldsymbol{w}_k, \boldsymbol{f}, \mathcal{M}) \geq \theta_1 \eta_1^2(\boldsymbol{w}_k, \boldsymbol{f}, \mathcal{T}_k) \tag{M}$$
$$\text{and } \eta_2^2(\boldsymbol{w}_k, \boldsymbol{\phi}_k, \mathcal{M}) \geq \theta_2 \eta_2^2(\boldsymbol{w}_k, \boldsymbol{\phi}_k, \mathcal{T}_k)$$

11:    **REFINE**: Bisect $K \in \mathcal{M}$ and their neighbors to form a conforming $\mathcal{T}_{k+1}$;
12:    $k \leftarrow k + 1$
13: **end while**
14: $N \leftarrow k$
15: Solve (3.5)–(3.6) on $\mathcal{T}_N$ to get $\boldsymbol{u}_N$.

The following two lemmas concern the contraction and the continuity of the estimators on two nested meshes, the proofs are standard in the AFEM literature thus omitted, the reader can refer to, e.g., [26,57].

Lemma 6.1 (Contraction of the estimators) *Let* $(\boldsymbol{w}_k, \boldsymbol{\phi}_k) \in \boldsymbol{V}_k^c \times \boldsymbol{V}_k^{\text{CR}}$ *and* $(\boldsymbol{w}_{k+1}, \boldsymbol{\phi}_{k+1}) \in \boldsymbol{V}_{k+1}^c \times \boldsymbol{V}_{k+1}^{\text{CR}}$ *be the solutions to* (3.1)–(3.4) *on triangulations* $\mathcal{T}_k$ *and* $\mathcal{T}_{k+1}$ *obtained through Algorithm 1,* $\rho = 1 - 2^{-1/3}$ *and there exists positive constants* $\beta_i \in (1 - \rho\theta_i, 1)$ *for* $i = 1, 2$ *such that*

$$\eta_{i,k}^2(\mathcal{T}_{k+1}) \leq \beta_i \eta_{i,k}^2(\mathcal{T}_k) - [\beta_i - (1 - \rho\theta_i)] \eta_{i,k}^2(\mathcal{T}_k).$$

Lemma 6.2 (Continuity of the estimator) *Under the same assumption with Lemma 6.1 then, then given positive constants* $\delta_i \in (0, 1)$ *for* $i = 1, 2$,

$$\eta_{1,k+1}^2(\mathcal{T}_{k+1}) \leq (1 + \delta_1) \eta_{1,k}^2(\mathcal{T}_{k+1}) + \frac{C_1}{\delta_1} r_{k+1}^2,$$

$$\text{and } \eta_{2,k+1}^2(\mathcal{T}_{k+1}) \leq (1 + \delta_2) \eta_{2,k}^2(\mathcal{T}_{k+1}) + \frac{C_2}{\delta_2} \left(h_{k+1}^2 r_{k+1}^2 + R_{k+1}^2 \right),$$

where C_i *depends on the shape-regularity of the mesh.*

Theorem 6.3 (Contraction) *Let* $(\boldsymbol{w}, \boldsymbol{\phi}) \in \boldsymbol{H}_0(\mathrm{curl}, \Omega) \times \boldsymbol{H}_0^1(\Omega; \mathbb{R}^3)$ *be the solutions to* (2.4)–(2.7) *without the Lagrange multipliers, and* $(\boldsymbol{w}_{k+1}, \boldsymbol{\phi}_{k+1}) \in \boldsymbol{V}_{k+1}^c \times \boldsymbol{V}_{k+1}^{CR}$ *and* $(\boldsymbol{w}_k, \boldsymbol{\phi}_k) \in \boldsymbol{V}_k^c \times \boldsymbol{V}_k^{CR}$ *be their approximations in problems* (3.1)–(3.4) *on* $\mathcal{T}_{k+1}$ *and* $\mathcal{T}_k$, *respectively. If* $\mathcal{T}_{k+1}$ *is a conforming refinement from* $\mathcal{T}_k$ *with* $h_{k+1} \leq h_k$, *then there exist* $\gamma_1, \gamma_2, \mu, \beta > 0$, *and* $0 < \alpha < 1$ *such that the AFEM in Algorithm* 1 *satisfies*

$$
\begin{aligned}
&|\boldsymbol{\phi} - \boldsymbol{\phi}_{k+1}|_{1,k+1}^2 + \mu h_{k+1}^2 \|\operatorname{curl}(\boldsymbol{w} - \boldsymbol{w}_{k+1})\|_0^2 \\
&\quad + \gamma_1 h_{k+1}^2 \eta_1^2(\boldsymbol{w}_{k+1}, \boldsymbol{f}, \mathcal{T}_{k+1}) + \gamma_2 \tilde{\eta}_2^2(\boldsymbol{\phi}_{k+1}, \boldsymbol{w}_{k+1}, \mathcal{T}_{k+1}) \\
&\leq \alpha \Big(|\boldsymbol{\phi} - \boldsymbol{\phi}_k|_{1,k}^2 + \mu h_k^2 \|\operatorname{curl}(\boldsymbol{w} - \boldsymbol{w}_k)\|_0^2 + \gamma_1 h_k^2 \eta_1^2(\boldsymbol{w}_k, \boldsymbol{f}, \mathcal{T}_k) + \gamma_2 \tilde{\eta}_2^2(\boldsymbol{\phi}_k, \boldsymbol{w}_k, \mathcal{T}_k) \Big)
\end{aligned}
$$

where

$$
\tilde{\eta}_2^2(\boldsymbol{w}_k, \boldsymbol{\phi}_k, \mathcal{T}_k) := \left(\eta_2^2(\boldsymbol{w}_k, \boldsymbol{\phi}_k, \mathcal{T}_k) + \beta \sum_{K \in \mathcal{T}_k} h_K^2 \|\operatorname{curl} \boldsymbol{w}_k\|_{0,K}^2 \right)
$$

is the modified estimator.

Proof First by the Galerkin orthogonality (3.7), we have $e_{k+1}^2 = e_k^2 - r_{k+1}^2$. Assuming that the constant in the quasi-orthogonality (5.9) is $\sqrt{C_Q/2}$, we have by Young's inequality for an $\epsilon \in (0, 1)$

$$
\begin{aligned}
E_{k+1}^2 &= E_k^2 - R_{k+1}^2 - 2\big(\nabla_{k+1}(\boldsymbol{\phi} - \boldsymbol{\phi}_{k+1}), \nabla_{k+1}(\boldsymbol{\phi}_{k+1} - \boldsymbol{\phi}_k)\big) \\
&\leq E_k^2 - R_{k+1}^2 + \sqrt{2C_Q}\big(h_k r_{k+1} + g_k(\mathcal{T}_k \backslash \mathcal{T}_{k+1})\big) E_{k+1} \\
&\leq E_k^2 - R_{k+1}^2 + \epsilon E_{k+1}^2 + \frac{C_Q}{\epsilon}\big(h_k^2 r_{k+1}^2 + g_k^2(\mathcal{T}_k \backslash \mathcal{T}_{k+1})\big).
\end{aligned} \tag{6.1}
$$

Now from Lemmas 6.1 and 6.2, and $h_{k+1} \leq h_k$, we choose δ_i $(i = 1, 2)$ such that $\beta_i := (1 - \rho\theta_i)(1 + \delta_i) \in (0, 1)$, we have

$$
\eta_{1,k+1}^2(\mathcal{T}_{k+1}) \leq \beta_1 \eta_{1,k}^2(\mathcal{T}_k) + \left[\delta_1 \beta_1 - (1 + \delta_1)\big(\beta_1 - (1 - \rho\theta_1)\big)\right] \eta_{1,k}^2(\mathcal{T}_k) + \frac{C_1}{\delta_1} r_{k+1}^2, \tag{6.2}
$$

and

$$
\begin{aligned}
\eta_{2,k+1}^2(\mathcal{T}_{k+1}) &\leq \beta_2 \eta_{2,k}^2(\mathcal{T}_k) + \left[\delta_2 \beta_2 - (1 + \delta_2)\big(\beta_2 - (1 - \rho\theta_2)\big)\right] \eta_{2,k}^2(\mathcal{T}_k) \\
&\quad + \frac{C_2}{\delta_2}\big(h_k^2 r_{k+1}^2 + R_{k+1}^2\big).
\end{aligned} \tag{6.3}
$$

Next for the element residual term in η_2 on each K we have:

$$
\begin{aligned}
\|\operatorname{curl} \boldsymbol{w}_{k+1}\|_{0,K}^2 &= \|\operatorname{curl} \boldsymbol{w}_k\|_{0,K}^2 - \|\operatorname{curl}(\boldsymbol{w}_k - \boldsymbol{w}_{k+1})\|_{0,K}^2 \\
&\quad - 2\big(\operatorname{curl} \boldsymbol{w}_{k+1}, \operatorname{curl}(\boldsymbol{w}_k - \boldsymbol{w}_{k+1})\big)_K.
\end{aligned}
$$

By the Young's inequality for a $\delta_3 \in (0, 1)$,

$$
(1 - \delta_3) \|\operatorname{curl} \boldsymbol{w}_{k+1}\|_{0,K}^2 \leq \|\operatorname{curl} \boldsymbol{w}_k\|_{0,K}^2 + \frac{1 - \delta_3}{\delta_3} \|\operatorname{curl}(\boldsymbol{w}_k - \boldsymbol{w}_{k+1})\|_{0,K}^2,
$$

and consequently applying similar techniques with Lemma 6.1 yields:

$$
(1 - \delta_3) g_{k+1}^2(\mathcal{T}_{k+1}) \leq g_k^2(\mathcal{T}_k) - \rho g_k^2(\mathcal{T}_k \backslash \mathcal{T}_{k+1}) + \frac{C_3}{\delta_3} h_{k+1}^2 r_{k+1}^2. \tag{6.4}
$$

To prove the contraction result, we define

$$\mathfrak{G}_{k+1} := (1 - \epsilon)E_{k+1}^2 + \mu h_{k+1}^2 e_{k+1}^2$$
$$+ \gamma_1 h_{k+1}^2 \eta_{1,k+1}^2(\mathcal{T}_{k+1}) + \gamma_2 \eta_{2,k+1}^2(\mathcal{T}_{k+1}) + (1 - \delta_3)\gamma_3 g_{k+1}^2(\mathcal{T}_{k+1})$$

and

$$\overline{\mathfrak{G}}_k := E_k^2 + \mu h_k^2 e_k^2$$
$$+ \gamma_1 \beta_1 h_k^2 \eta_{1,k}^2(\mathcal{T}_k) + \gamma_2 \beta_2 \eta_{2,k}^2(\mathcal{T}_k) + \gamma_3 g_k^2(\mathcal{T}_k).$$

Combining estimates (6.1), (6.2), (6.3) and (6.4) above,

$$\mathfrak{G}_{k+1} \le \overline{\mathfrak{G}}_k - \left(1 - \frac{\gamma_2 C_2}{\delta_2}\right) R_{k+1}^2$$
$$- \left(\mu - \frac{C_Q}{\epsilon} - \sum_{j=1}^{3} \frac{\gamma_j C_j}{\delta_j}\right) h_k^2 r_{k+1}^2$$
$$+ \gamma_1 h_k^2 \Big[\delta_1 \beta_1 - (1 + \delta_1)(\beta_1 - (1 - \rho\theta_1))\Big] \eta_{1,k}^2(\mathcal{T}_k) \tag{6.5}$$
$$+ \gamma_2 \Big[\delta_2 \beta_2 - (1 + \delta_2)(\beta_2 - (1 - \rho\theta_2))\Big] \eta_{2,k}^2(\mathcal{T}_k)$$
$$- \left(\gamma_3 \rho - \frac{C_Q}{\epsilon}\right) g_k^2(\mathcal{T}_k \backslash \mathcal{T}_{k+1}).$$

The constants are formulated such that all terms on the right hand side except the first in the inequality above vanish for a fixed $\epsilon \in (0, 1)$, which is determined later. To this end, aside from the choice of δ_i $(i = 1, 2)$ above, we choose γ_2 and γ_3 to be

$$\gamma_2 = \frac{\delta_2}{C_2}, \quad \text{and} \quad \gamma_3 = \frac{C_Q}{\rho\epsilon}, \tag{6.6}$$

and γ_1 is a free constant. Additionally, μ is free as well, and is to be chosen sufficiently large such that the following holds regardless of what values ϵ and δ_3 take

$$\mu - \frac{C_Q}{\epsilon} - \sum_{j=1}^{3} \frac{\gamma_j C_j}{\delta_j} \ge 0.$$

Consequently, (6.5) becomes $\mathfrak{G}_{k+1} \le \overline{\mathfrak{G}}_k$. For an $\alpha \in (0, 1)$ we rewrite the right hand side of (6.5) as

$$\overline{\mathfrak{G}}_k = \alpha \mathfrak{G}_k + \mathfrak{R}_k,$$

where

$$\mathfrak{R}_k := \big(1 - \alpha(1 - \epsilon)\big)E_k^2 + \mu(1 - \alpha)h_k^2 e_k^2$$
$$+ \gamma_1(\beta_1 - \alpha)h_k^2 \eta_{1,k}^2(\mathcal{T}_k) + \gamma_2(\beta_2 - \alpha)\eta_{2,k}^2(\mathcal{T}_k) + \gamma_3\big(1 - \alpha(1 - \delta_3)\big)g_k^2(\mathcal{T}_k).$$

It suffices to show that for the constants chosen and to be determined, there exists an $\alpha \in (0, 1)$ such that $\mathfrak{R}_k \le 0$. Now assuming that the constant in the reliability estimate (4.5) is $\sqrt{C_R/2}$, and the fact that $g_k(\mathcal{T}_k) \le \eta_{2,k}(\mathcal{T}_k)$ we have

$$\mathfrak{R}_k \le \big(h_k^2 \eta_{1,k}^2(\mathcal{T}_k) + \eta_{2,k}^2(\mathcal{T}_k)\big)\Big[C_R\big(1 - \alpha(1 - \epsilon) + \mu(1 - \alpha)\big)$$
$$+ (\beta_1 - \alpha)\gamma_1 + (\beta_2 - \alpha)\gamma_2 + \gamma_3\big(1 - \alpha(1 - \delta_3)\big)\Big].$$

It is straightforward to verify the second term on the right hand side above vanishes when letting

$$\alpha := \frac{C_R(1+\mu) + \gamma_1\beta_1 + \gamma_2\beta_2 + \gamma_3}{C_R(1+\mu-\epsilon) + \gamma_1 + \gamma_2 + \gamma_3(1-\delta_3)} > 0. \tag{6.7}$$

To make $\alpha < 1$, by (6.6), the following inequality is needed:

$$\epsilon C_R + \delta_3 \frac{C_Q}{\rho\epsilon} < \gamma_1(1-\beta_1) + \gamma_2(1-\beta_2). \tag{6.8}$$

Choosing

$$\delta_3 = \rho\epsilon^2 \quad \text{and} \quad \gamma_1 = \frac{\gamma_2\beta_2}{1-\beta_1},$$

we have (6.8) holds with

$$0 < \epsilon < \min\left\{\frac{\delta_2}{C_2(C_R+C_Q)}, 1\right\}$$

and thus α defined in (6.7) is in $(0, 1)$. As a result, $\mathfrak{G}_{k+1} \leq \alpha\mathfrak{G}_k$ is shown, and finally the theorem follows by acknowledging that $g_k(\mathcal{T}_k)$ is a part of $\eta_{2,k}(\mathcal{T}_k)$. $\qquad\square$

7 Numerical Examples

The numerical experiments in this section, as well as in Sect. 3.2, are carried out using iFEM [14]. The code used for this paper is publicly available at https://github.com/lyc102/ifem/tree/master/research/quadCurl. The linear systems for the Stokes problem originated from (3.3)–(3.4) are solved using MINRES with a diagonal preconditioner, the inverse of the Schur complement of the lower right block can be efficiently approximated by a few V-cycles. For the discretized Maxwell saddle problems (3.1)–(3.2) and (3.5)–(3.6), we use the multigrid method for Hodge Laplacian to solve a block factorization; see [17, Section 4.4].

    We mainly compare the performance of the adaptive algorithm under the proposed separate marking strategy (M) in Algorithm 1 versus two single marking strategies: A minimum $\mathcal{M} \subseteq \mathcal{T}_k$ is sought such that

$$\eta^2(\boldsymbol{w}_h, \boldsymbol{\phi}_h, \boldsymbol{f}, \mathcal{M}) \geq \theta\eta^2(\boldsymbol{w}_h, \boldsymbol{\phi}_h, \boldsymbol{f}, \mathcal{T}_k), \tag{M1}$$

or

$$\widetilde{\eta}^2(\boldsymbol{w}_h, \boldsymbol{\phi}_h, \boldsymbol{f}, \mathcal{M}) \geq \theta\widetilde{\eta}^2(\boldsymbol{w}_h, \boldsymbol{\phi}_h, \boldsymbol{f}, \mathcal{T}_k), \tag{M2}$$

where η is defined as

$$\eta^2(\boldsymbol{w}_h, \boldsymbol{\phi}_h, \boldsymbol{f}, \mathcal{M}) := \eta_1^2(\boldsymbol{w}_h, \boldsymbol{f}, \mathcal{M}_h) + \eta_2^2(\boldsymbol{\phi}_h, \boldsymbol{w}_h, \mathcal{M}), \tag{7.1}$$

and $\widetilde{\eta}(\boldsymbol{w}_h, \boldsymbol{\phi}_h, \boldsymbol{f}, \mathcal{M})$ is defined by the L^2-sum of the weighted η_1 and η_2:

$$
\begin{aligned}
\widetilde{\eta}^2(\boldsymbol{w}_h, \boldsymbol{\phi}_h, \boldsymbol{f}, \mathcal{M}) := &\sum_{K\in\mathcal{M}} h_K^4 \|\boldsymbol{f}\|_{0,K}^2 + \sum_{F\in\mathcal{F}_h^i(\mathcal{M})} h_F^3 \|[\![(\operatorname{curl}\boldsymbol{w}_h) \times \boldsymbol{n}_F]\!]\|_{0,F}^2 \\
&+ \sum_{K\in\mathcal{M}} h_K^2 \|\operatorname{curl}\boldsymbol{w}_h\|_{0,K}^2 + \sum_{F\in\mathcal{F}_h(\mathcal{M})} h_F \|[\![\boldsymbol{n}_F \times (\boldsymbol{\nabla}_h\boldsymbol{\phi}_h)]\!]\|_{0,F}^2.
\end{aligned}
\tag{7.2}
$$

On a uniform mesh, $\widetilde{\eta}^2$ can be viewed as approximately $h^2\eta_1^2 + \eta_2^2$.
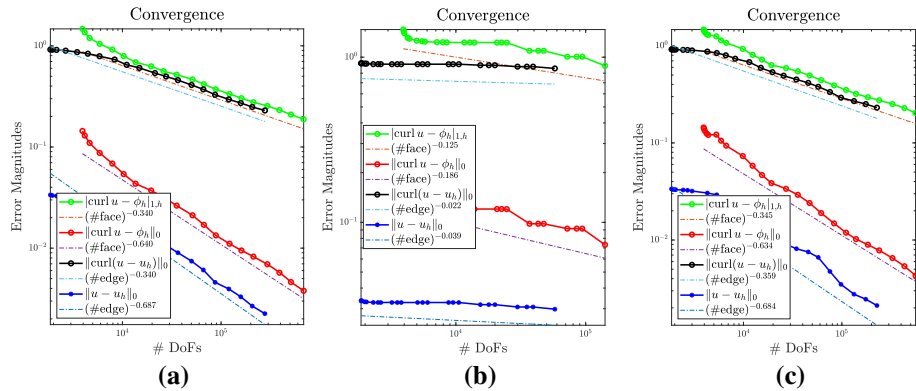
Fig. 3 The convergence results for AFEM 1 using different marking strategies: **a** separate marking for η_1 and η_2. **b** single marking for η. (c) single marking for $\widetilde{\eta}$

To demonstrate the reason why we opt for the proposed separate marking strategy (M), and not single markings such as (M1) and (M2), we construct a toy example using $\boldsymbol{u} = \operatorname{curl}\langle 0, 0, \mu\rangle$ for a potential function $\mu = r^{19/6}\sin(2\theta/3)$ in the cylindrical coordinate as in Sect. 3.2 example 2 on an L-shaped domain. In this case we have a regular $\boldsymbol{\phi} = \operatorname{curl}\boldsymbol{u} \in H^{13/6-\epsilon}(\Omega)$ while $\boldsymbol{w}$ has a mild singularity near the nonconvex corner.

The results for the convergence of Algorithm 1 using marking strategies (M), (M1), and (M2) can be found in Figs. 3a–c, respectively.

Using the proposed marking (M), we obtain the desired optimal convergence for $|\boldsymbol{\phi}_h - \operatorname{curl}\boldsymbol{u}|_{1,h}$ being optimal in that the convergence is at the rate of "linear" $\approx \#(\text{DoF})^{-1/3}$. Additionally, $\|\boldsymbol{\phi}_h - \operatorname{curl}\boldsymbol{u}\|_0$ and $\|\boldsymbol{u} - \boldsymbol{u}_h\|_0$ converge "quadratically", i.e., in the order of approximately $\#(\text{DoF})^{-2/3}$ even though the error estimator's reliability and efficiency are not directly measured in those norms. In this experiment, $\theta_1 = 0.5$ and $\theta_2 = 0.3$.

Using marking (M1) with $\theta = 0.3$, if η_1 is unweighted in the η in (7.1), due to $\boldsymbol{w}$ being singular while $\boldsymbol{\phi}$ being regular, thanks to η_1 being locally efficient, the marked elements are dominantly concentrated on which η_1 are large. As a result, marking (M1) drives the AFEM algorithm favoring reducing the error for $\boldsymbol{w}$, while the errors in approximating $\boldsymbol{\phi}$ and $\boldsymbol{u}$ barely change (Fig. 3b). Fortunately, due to the regularity lifting effect from $\boldsymbol{w}_h$ being the data for the problem of $\boldsymbol{\phi}_h$ (cf. Lemma 3.3), to achieve the optimal rate of convergence, $\boldsymbol{w}_h$ does not have to be approximated to the same precision with $\boldsymbol{\phi}_h$.

If marking (M2) with $\theta = 0.3$ is used where η_1 is locally weighted by the mesh size h_K, the optimal rates of convergence is restored. However, one does benefit from choosing different marking parameters for approximating $\boldsymbol{w}$ and $\boldsymbol{\phi}$ due to the regularity difference (see e.g., [18]). Moreover, one does not have the Galerkin orthogonality for $\|\operatorname{curl}(\boldsymbol{w} - \boldsymbol{w}_h)\|$ to exploit in the proof of the contraction in Theorem 6.3, because the consecutive difference is measured under a norm weighted by the mesh size. As a result, it needs new tools that are not available in any of the current literature to prove a similar contraction result when the local error indicator is further weighted by the local mesh size h_K.

References

1. Arnold, D.N.: Finite element exterior calculus, volume 93 of CBMS-NSF Regional Conference Series in Applied Mathematics. Society for Industrial and Applied Mathematics (SIAM), Philadelphia, PA (2018)
2. Arnold, D.N., Falk, R.S., Winther, R.: Finite element exterior calculus, homological techniques, and applications. Acta Numer. **15**, 1–155 (2006)
3. Arnold, D.N., Hu, K.: Complexes from complexes. Found. Comput. Math. **1–36**,(2021)
4. Beck, R., Hiptmair, R., Hoppe, R.W., Wohlmuth, B.: Residual based a posteriori error estimators for Eddy current computation. M2AN Math. Model. Numer. Anal. **34**, 159–182 (2000)
5. Biskamp, D.: Magnetic reconnection in plasmas. Astrophys. Space Sci. **242**(1–2), 165–207 (1996)
6. Boffi, D., Brezzi, F., Fortin, M.: Mixed Finite Element Methods and Applications. Springer, Heidelberg (2013)
7. Brenner, S.C.: Two-level additive Schwarz preconditioners for nonconforming finite element methods. Math. Comp. **65**(215), 897–921 (1996)
8. Brenner, S.C.: Poincaré-Friedrichs inequalities for piecewise H^1 functions. SIAM J. Numer. Anal. **41**(1), 306–324 (2003)
9. Brenner, S.C., Scott, R.: The Mathematical Theory of Finite Element Methods, vol. 15. Springer, Berlin (2008)
10. Brenner, S.C., Sun, J., Sung, L.-Y.: Hodge decomposition methods for a quad-curl problem on planar domains. J. Sci. Comput. **73**(2), 495–513 (2017)
11. Cai, Z., Cao, S.: A recovery-based a posteriori error estimator for H(curl) interface problems. Comput. Methods Appl. Mech. Eng. **296**, 169–195 (2015)
12. Cakoni, F., Haddar, H.: A variational approach for the solution of the electromagnetic interior transmission problem for anisotropic media. Inverse Probl. Imag. **1**(3), 443 (2007)
13. Chacón, L., Simakov, A.N., Zocco, A.: Steady-state properties of driven magnetic reconnection in 2d electron magnetohydrodynamics. Phys. Rev. Lett. **99**(23), 235001 (2007)
14. Chen, L.: iFEM: an integrated finite element methods package in MATLAB. University of California at Irvine (2009)
15. Chen, L., Huang, X.: Decoupling of mixed methods based on generalized Helmholtz decompositions. SIAM J. Numer. Anal. **56**(5), 2796–2825 (2018)
16. Chen, L., Wu, Y.: Convergence of adaptive mixed finite element methods for the Hodge Laplacian equation: without harmonic forms. SIAM J. Numer. Anal. **55**(6), 2905–2929 (2017)
17. Chen, L., Wu, Y., Zhong, L., Zhou, J.: Multigrid preconditioners for mixed finite element methods of the vector Laplacian. J. Sci. Comput. **77**(1), 101–128 (2018)
18. Chen, Z., Dai, S.: On the efficiency of adaptive finite element methods for elliptic problems with discontinuous coefficients. SIAM J. Sci. Comput. **24**(2), 443–462 (2002)
19. Cochez-Dhondt, S., Nicaise, S.: Robust a posteriori error estimation for the Maxwell equations. Comput. Methods Appl. Mech. Engrg. **196**, 2583–2595 (2007)
20. Crouzeix, M., Raviart, P.-A.: Conforming and nonconforming finite element methods for solving the stationary Stokes equations. I. Rev. Française Automat. Informat. Recherche Opérationnelle Sér. Rouge **7**(R–3), 33–75 (1973)
21. Dari, E., Durán, R., Padra, C.: Error estimators for nonconforming finite element approximations of the Stokes problem. Math. Comp. **64**(211), 1017–1033 (1995)
22. Dari, E., Duran, R., Padra, C., Vampa, V.: A posteriori error estimators for nonconforming finite element methods. RAIRO Modél. Math. Anal. Numér. **30**(4), 385–400 (1996)
23. Demlow, A., Hirani, A.N.: A posteriori error estimates for finite element exterior calculus: the de Rham complex. Found. Comput. Math. **14**(6), 1337–1371 (2014)
24. Girault, V., Raviart, P.-A.: Finite Element Methods for Navier–Stokes Equations: Theory and Algorithms. Springer, Berlin (1986)
25. Hong, Q., Hu, J., Shu, S., Xu, J.: A discontinuous galerkin method for the fourth-order curl problem. J. Comput. Math. **30**(6), 565–578 (2012)
26. Hu, J., Xu, J.: Convergence and optimality of the adaptive nonconforming linear element method for the Stokes problem. J. Sci. Comput. **55**(1), 125–148 (2013)
27. Hu, K., Zhang, Q., Zhang, Z.: A family of finite element Stokes complexes in three dimensions (2020). arXiv preprint arXiv:2008.03793
28. Hu, K., Zhang, Q., Zhang, Z.: Simple curl-curl-conforming finite elements in two dimensions. SIAM J. Sci. Comput. **42**(6), A3859–A3877 (2020)
29. Huang, J., Huang, X.: Local and parallel algorithms for fourth order problems discretized by the Morley–Wang–Xu element method. Numer. Math. **119**(4), 667–697 (2011)

30. Huang, X.: Nonconforming finite element Stokes complexes in three dimensions (2020). arXiv preprint arXiv:2007.14068

31. Kikuchi, F.: Mixed formulations for finite element analysis of magnetostatic and electrostatic problems. Japan J. Appl. Math. **6**(2), 209 (1989)

32. Kikuchi, F.: On a discrete compactness property for the nédélec finite elements. Journal of the Faculty of Science, the University of Tokyo. Sect. 1 A **36**(3), 479–490 (1989)

33. Kingsep, A., Chukbar, K., Yankov, V.: Electron magnetohydrodynamics. Rev. Plasma Phys. **16**,(1990)

34. Maz'ya, V., Rossmann, J.: Elliptic Equations in Polyhedral Domains, Mathematical surveys and monographs. American Mathematical Society (2010)

35. Monk, P.: Finite element methods for Maxwell's equations. Numerical Mathematics and Scientific Computation. Oxford University Press, New York (2003)

36. Monk, P., Sun, J.: Finite element methods for maxwell's transmission eigenvalues. SIAM J. Sci. Comput. **34**(3), B247–B264 (2012)

37. Nédélec, J.-C.: Mixed finite elements in R^3. Numer. Math. **35**(3), 315–341 (1980)

38. Nédélec, J.-C.: A new family of mixed finite elements in R^3. Numer. Math. **50**(1), 57–81 (1986)

39. Neilan, M.: Discrete and conforming smooth de rham complexes in three dimensions. Math. Comp. **84**(295), 2059–2081 (2015)

40. Nicaise, S.: Singularities of the quad curl problem. J. Differ. Equ. **264**(8), 5025–5069 (2018)

41. Raviart, P.-A., Thomas, J.M.: A mixed finite element method for 2nd order elliptic problems. In: Mathematical aspects of finite element methods (Proc. Conf., Consiglio Naz. delle Ricerche (C.N.R.), Rome, 1975), Lecture Notes in Math., vol. 606, pp. 292–315. Springer, Berlin (1977)

42. Schöberl, J.: A posteriori error estimates for Maxwell equations. Math. Comp. **77**(262), 633–649 (2008)

43. Scott, L.R., Zhang, S.: Finite element interpolation of nonsmooth functions satisfying boundary conditions. Math. Comp. **54**(190), 483–493 (1990)

44. Simakov, A.N., Chacon, L.: Quantitative analytical model for magnetic reconnection in hall magnetohydrodynamics. Phys. Plasmas **16**(5), 055701 (2009)

45. Sun, J.: A mixed fem for the quad-curl eigenvalue problem. Numer. Math. **132**(1), 185–200 (2016)

46. Sun, J., Zhang, Q., Zhang, Z.: A curl-conforming weak galerkin method for the quad-curl problem. BIT Numer. Math. **59**(4), 1093–1114 (2019)

47. Sweet, P.A.: The Neutral Point Theory of Solar Flares. In: Lehnert, B. (ed) Electromagnetic Phenomena in Cosmical Physics, vol. 6, p. 123 (1958)

48. Verfürth, R.: A posteriori error estimators for the stokes equations ii non-conforming discretizations. Numer. Math. **60**(1), 235–249 (1991)

49. Wang, C., Sun, Z., Cui, J.: A new error analysis of a mixed finite element method for the quad-curl problem. Appl. Math. Comput. **349**, 23–38 (2019)

50. Wang, L., Zhang, Q., Sun, J., Zhang, Z.: A priori and a posteriori error estimates for the quad-curl eigenvalue problem (2020). arXiv preprint arXiv:2007.01330

51. Zhang, Q., Wang, L., Zhang, Z.: H (curl^2)-conforming finite elements in 2 dimensions and applications to the quad-curl problem. SIAM J. Sci. Comput. **41**(3), A1527–A1547 (2019)

52. Zhang, Q., Zhang, Z.: Curl-curl conforming elements on tetrahedra (2020). arXiv preprint arXiv:2007.10421

53. Zhang, S.: Mixed schemes for quad-curl equations. ESAIM Math. Model. Numer. Anal. **52**(1), 147–161 (2018)

54. Zhao, J., Zhang, B.: The curl-curl conforming virtual element method for the quad-curl problem. Math. Models Methods Appl. Sci. **31**(8), 1659–1690 (2021)

55. Zheng, B., Hu, Q., Xu, J.: A nonconforming finite element method for fourth order curl equations in $\mathbb{R}^3$. Math. Comp. **80**(276), 1871–1886 (2011)

56. Zheng, W., Chen, Z., Wang, L.: An adaptive finite element method for the h-ψ formulation of time-dependent eddy current problems. Numer. Math. **103**(4), 667–689 (2006)

57. Zhong, L., Chen, L., Shu, S., Wittum, G., Xu, J.: Convergence and optimality of adaptive edge finite element methods for time-harmonic Maxwell equations. Math. Comp. **81**(278), 623–642 (2012)

58. Zhong, L., Shu, S., Chen, L., Xu, J.: Convergence of adaptive edge finite element methods for H(**curl**)-elliptic problems. Numer. Linear Algebra Appl. **17**(2–3), 415–432 (2010)

59. Zhong, L., Shu, S., Wittum, G., Xu, J.: Optimal error estimates for nedelec edge elements for time-harmonic maxwell's equations. J. Comput. Math. **563–572**,(2009)